Research paper

# Synthesis of podophyllotoxin linked β-carboline congeners as potential anticancer agents and DNA topoisomerase II inhibitors

Manda Sathish [a], Botla Kavitha [b], V. Lakshma Nayak [a], Yellaiah Tangella [a], Ayyappan Ajitha [c], Shalini Nekkanti [b], Abdullah Alarifi [d], Nagula Shankaraiah [b, ***], Narayana Nagesh [c, **], Ahmed Kamal [a, b, d, e, *]

[a] Medicinal Chemistry and Pharmacology, CSIR-Indian Institute of Chemical Technology, Hyderabad 500 007, India
[b] Department of Medicinal Chemistry, National Institute of Pharmaceutical Education and Research (NIPER), Hyderabad 500 037, India
[c] CSIR-Centre for Cellular and Molecular Biology, Hyderabad 500 007, India
[d] Catalytic Chemistry Research Chair, Chemistry Department, College of Science, King Saud University, Riyadh 11451, Saudi Arabia
[e] School of Pharmaceutical Education and Research (SPER), Jamia Hamdard University, New Delhi 110 062, India

## ARTICLE INFO

## ABSTRACT

A series of new podophyllotoxin linked β-carboline congeners have been synthesized by coupling various substituted β-carboline acids with 4β-aminopodophyllotoxin. Evaluation of their anticancer activity against a panel of human cancer cell lines such as lung cancer (A549), prostate cancer (DU-145), MDA MB-231 (breast cancer), HT-29 (colon cancer) and HeLa (cervical cancer) suggested that **7i** and **7j** are the most cytotoxic compounds with IC$_{50}$ values of $1.07 \pm 0.07$ μM and $1.14 \pm 0.16$ respectively against DU-145 cell line. Further, detailed biological studies such as cell cycle analysis, topoisomerase II inhibition, Comet assay, DNA binding studies and docking studies have revealed that these congeners are DNA interacting topoisomerase II inhibitors.

## 1. Introduction

Topoisomerase-II (topo II) is a vital nuclear enzyme involved in various DNA processes and also a major target for many drugs currently used in cancer chemotherapy [1]. Based on their mechanism of action, these drugs can be classified into catalytic inhibitory compounds (CICs) and interfacial poisons (IFPs) [2]. The CICs target the N-terminal ATPase domain of topo II and inhibit it at an initial stage by stabilizing the enzyme-ligand-DNA ternery complex eg: ICRF 193 (**I**, Fig. 1) [3]. On the other hand, IFPs initiate the cleavage reaction and stop the re-ligation of DNA, which leads to apoptosis eg: doxorubicin [4] (**II**) and amsacrine [2] (**III**) Fig. 1.

Podophyllotoxin (**IV**) is a well-known natural lignan which is extracted from the roots of *Podophyllotoxin peltatum*. Podophyllotoxin (**IV**) and its derivatives are potent anticancer agents acting through diverse mechanisms; the former is an inhibitor of microtubule assembly while the latter are DNA interacting agents and topoisomerase inhibitors [5,6]. Many research groups have explored the structure activity relationships (SARs) of podophyllotoxin based on the results from several modifications of the ring systems (ring A, B, C, D and E) of podophyllotoxin (**IV**, Fig. 1) [7]. Among all the structural changes, the modification at the C-4 position of C-ring has received great attention and the resulting derivatives displayed dramatic improvement in DNA topo II inhibition with significant anticancer activity [7]. These studies have led to the development of semi-synthetic podophyllotoxin derivatives such as etoposide (**F**) and teniposide (**G**) [8,9]. From the SAR studies, it is clear that the podophyllotoxin derivatives in subcellular level bind selectively to the colchicine binding site of tubulin, and inhibit the formation of microtubule. Interestingly, etoposide (**V**) as well as teniposide (**VI**) do not affect the tubulin polymerization and are reported as irreversible DNA topo II inhibitors (Fig. 1) which

* Corresponding author. Medicinal Chemistry and Pharmacology, CSIR-Indian Institute of Chemical Technology, Hyderabad 500 007, India. Tel.: +91 40 27193157; fax: +91 40 27193189.
** Corresponding author.
*** Corresponding author.
E-mail addresses: shankar@niperhyd.ac.in (N. Shankaraiah), nagesh@ccmb.res.in (N. Nagesh), ahmedkamal@iict.res.in (A. Kamal).
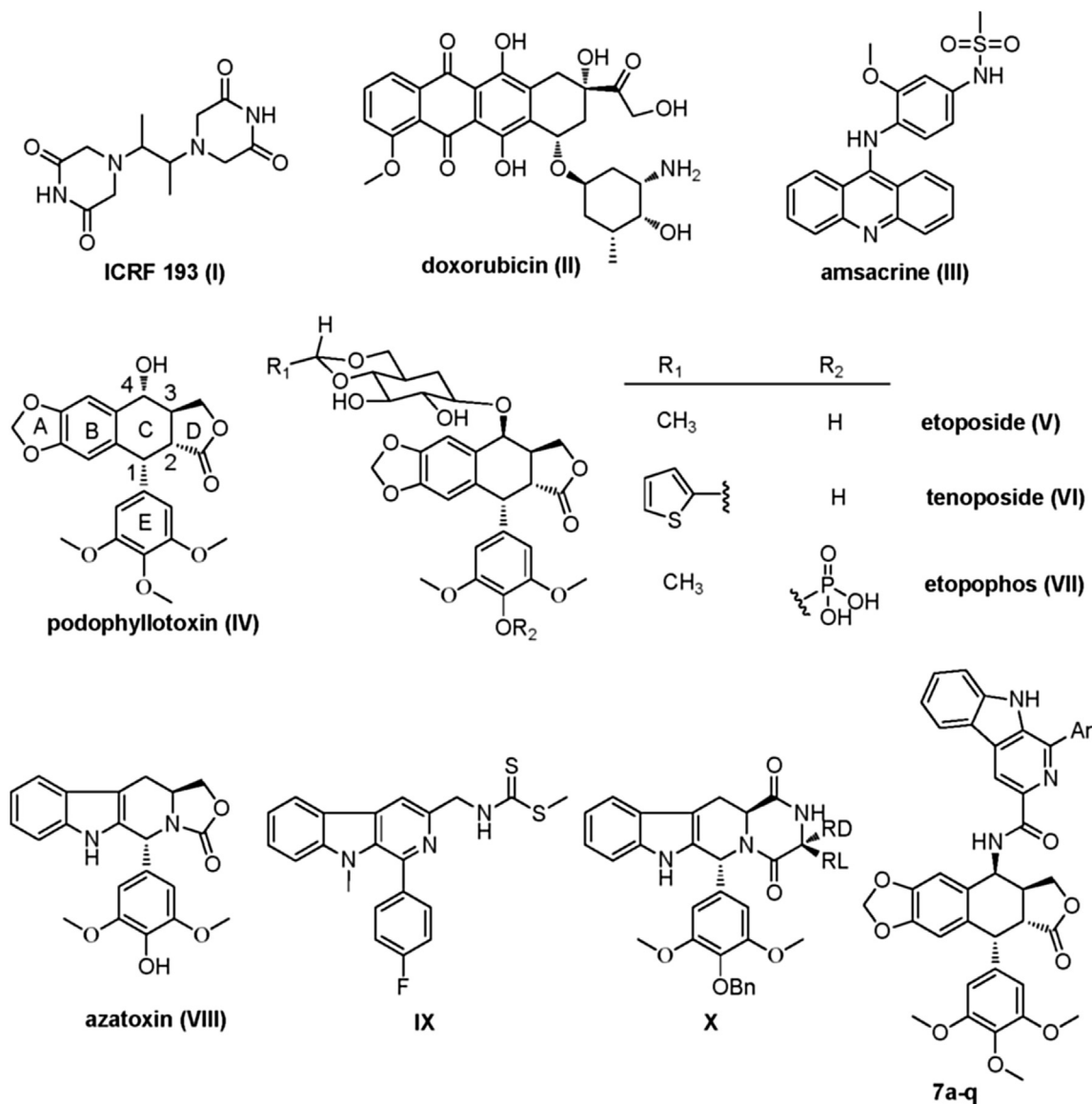
**Fig. 1.** Various type of DNA topo II inhibitors: Podophyllotoxin derivatives (**V**, **VI** and **VII**), β-carboline derivatives (**VIII**, **IX** and **X**) and synthesized podophyllotoxin-linked β-carboline congeners (**7a–q**).

indicates that bulky groups like sugar moiety at C-4 position on the C-ring of podophyllotoxin may be responsible for the topo II inhibition [10]. Due to the poor solubility of etoposide, a phosphate ester prodrug has been developed (etopophos (**VII**), Fig. 1) [11] which is used in chemotherapy for Ewing's sarcoma, Kaposi's sarcoma, testicular cancer, lung cancer, lymphoma, glioblastoma multiforme and nonlymphocytic leukemia. Although numerous anticancer drugs are currently in use, many side effects like low blood pressure, hair loss, diarrhea, etc were accompanied with these drugs [12]. Hence, development of new cancer chemotherapeutic drugs with fewer side effects is highly desirable in the drug discovery process.

β-Carboline alkaloids are another interesting class of molecules with a wide variety of medicinal properties including anticancer activity [13]. Small molecules with β-carboline scaffold such as Harman, harmine, norharman and harmaline are isolated from *Peganum harmala* (Zygophillaceae, Syrian Rue) [14]. These molecules basically possess tricyclic planar structures with suitable features for DNA interaction and enzyme inhibition activities like

topoisomerase inhibition [15]. Moreover, they produce their anti-cancer effect through different modes of action, such as interacting with DNA (intercalation with DNA or external binding to DNA) [16], MK-2 [17], DNA topo inhibition [18], kinesin Eg5 [19] and CDK [20]. However, DNA interactive topoisomerase inhibition has been studied widely and gained much significance in cancer chemotherapy as many of the anticancer drugs currently in use display these mechanisms of action [21]. Azatoxin, a tetrahydro-β-carboline was rationally designed to inhibit topo II and binds to DNA in a non-intercalative fashion [22]. Macdonald et al. [22] have synthesized structurally azatoxin related amino acid linked β-carboline derivatives, which inhibit topo II mediated DNA relaxation. Recently, we have also reported dithiocarbamate linked β-carboline derivatives as DNA interactive topo II inhibitors with apoptosis ability [23a].

In search for newer anticancer agents with topoisomerase inhibition and in continuation of our efforts towards search for new chemical entities (NCEs) in drug discovery, we replaced the sugar moiety of etoposide with other bulky moieties like β-carboline and

envisioned to generate new conjugates with enhanced cytotoxic activity as well as DNA topo II inhibition. Thus, we describe the synthesis of new podophyllotoxin linked β-carboline congeners (**7a–q**) by coupling of β-carboline acids with 4β-amino-podophyllotoxin through simple amidation (Fig. 2). In this regard, we have synthesized **7a–q** and evaluated them for their cytotoxic activity, cell cycle analysis, DNA topo II inhibition, DNA binding affinity and molecular docking studies.

## 2. Results and discussion

### 2.1. Chemistry

The synthesis of podophyllotoxin linked β-carboline congeners (**7a–q**) have been discussed in Schemes 1 and 2. The intermediate β-carboline-3-carboxylic acids **5a–q** have been synthesized as shown in Scheme 1. The L-tryptophan methyl ester (**2**) was prepared from L-tryptophan (**1**) by employing $SOCl_2$. Next, Pictet-Spengler condensation of **2** with a variety of substituted benzaldehydes gave the corresponding methyl tetrahydro-β-carboline-3-carboxylates **3a–q** which were used directly for the aromatization by using trichloroisocyanuric acid (TCICA) to afford the methyl-β-carboline-3-carboxylates **4a−q**. These are further hydrolyzed in the presence of aqueous NaOH solution to get β-carboline acids **5a−q** in good yields and were employed in the final peptide coupling reaction.

Finally, the synthesis of the target podophyllotoxin linked β-carboline congeners **7a–q** have been achieved by the reaction of the intermediates **5a−q** with 4β-aminopodophyllotoxin (**6**) [23b] in presence of peptide coupling reagents such as EDCI and HOBt (Scheme 2).

### 2.2. Evaluation of biological activity

#### 2.2.1. Cytotoxicity

The podophyllotoxin-linked β-carboline congeners **7a–q** have been initially assayed for their *in vitro* cytotoxic activity against selected human cancer cell lines namely A549 (lung cancer), DU-145 (prostate cancer), MDA MB-231 (breast cancer), HT-29 (colon cancer) and HeLa (cervical cancer) using MTT assay [24]. All the congeners displayed moderate to good cytotoxicity and most of these demonstrate high cytotoxicity compared to doxorubicin, etoposide, podophyllotoxin and showed cytotoxicity selectively against DU-145 cells (Table 1). However, majority of these congeners such as **7d**, **7e** and **7i–7q** have exhibited sensible cytotoxicity with $IC_{50}$ values of <10 μM against DU-145 cells. Moreover, the

congeners **7i–7p** were found to be considerably cytotoxic with $IC_{50}$ value of <5 μM. Interestingly, the congeners **7i** and **7j** showed promising cytotoxicity with $IC_{50}$ value of 1.07 and 1.14 μM respectively against DU-145 cells. Further to evaluate the effect of active congeners **7i** and **7j,** cell cycle analysis, topo II inhibitory assay, DNA interaction studies and molecular docking studies were carried out.

#### 2.2.2. Cell cycle analysis

In order to substantiate the results obtained from MTT assay as well as to understand the effect of **7i** and **7j** on cell cycle progression, cell cycle assay was performed. On treatment of DU-145 cells with 1.0 μM concentration of each congener **7i** and **7j** for 48 h, significant increment in population of cells at S phase and $G_2/M$ phase ($\approx 41\%$ and $\approx 29\%$ respectively) was observed and compared to control cells ($\approx 25\%$ and $\approx 22\%$). However, moderate accumulation of cells in $subG_1$ phase (from $\approx 2\%$ to 11%) and extreme decrement of cells in $G_0/G_1$ phase ($\approx 51\%$ to $\approx 19\%$) was also observed. Moreover, the extent of population of cells at S and $G_2/M$ is slightly high with **7i** compared to **7j**. The high accumulation of cells in S and $G_2/M$ phase on treatment with **7i** and **7j** indicates their ability to stop cycle at cell division stage. Based on the results observed, the active congeners **7i** and **7j** efficiently arrested the cell cycle at S and $G_2/M$ phase. As reported earlier [25], the molecules that inhibit cell cycle at S and $G_2/M$ phase could effectively inhibit topoisomerase II and lead to apoptosis of cancer cell. The cell cycle histograms obtained for DU-145 on treatment of **7i** and **7j** at 1.0 μM concentrations each are shown in Fig. 3 and the results are tabulated in Table 2.

#### 2.2.3. DNA topoisomerase II inhibition assay

The enzymes which control the topology of DNA are called topoisomerases and play a crucial role in several important processes such as DNA replications, transcription, segregation and recombination [26]. Basically, two classes of topoisomerases are known: type I and type II topoisomerases. The type I topoisomerase known to make nicks on the single strand of DNA whereas type II topoisomerases are familiar for making nicks on both strands of DNA. The compounds that interfere with DNA topo II, inhibit the enzyme activity and stop the DNA replication which ultimately leads to cell death [27a]. Topo II inhibition assay was performed using Topo II Drug Screening Kit (TG 1009, Topogen, USA). In this present study, catenated DNA and topo II enzyme (5 units) were incubated with 10 μM etoposide for 30 min (lane 5, Fig. 4) and this was considered as positive control. In the control lane a linear DNA formation was observed, indicating that it catalyses the cleavage and inhibit the DNA resealing process. This indicates that etoposide functions as an interfacial poison (IFP). The kDNA which is catenated remained near the well itself (lane 1, Fig. 4) and upon addition of 5 units of topo II the catenated kDNA has converted mostly to linear form (line 2, Fig. 4). The catenated kDNA under similar conditions was incubated with topo II and 10 μM of **7i** and **7j** (lane 3 and 4 respectively, Fig. 8), did not observe the formation of linear DNA. However, most of the catenated DNA remained in the well without entering into the gel, signifies the formation of stable topo II-kDNA-**7i/7j** ternary complex. Hence, it indicates that **7i** and **7j** congeners will interfere with topo II enzyme of catalytic activity and these are considered as CIC. This assay indicates that the **7i** and **7j** would interfere with catalytic activity of topo II enzyme and act as catalytic inhibitors.

#### 2.2.4. Comet assay

The topoisomerase II inhibition assay indicate that **7i** and **7j** are efficient in inhibiting the activity of topoisomerase II. To study the role of these congeners in fragmenting the DNA, a single cell based assay namely comet assay was performed. It is used to detect
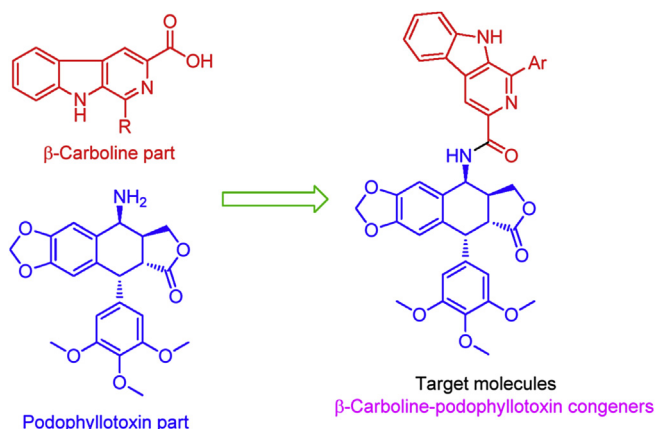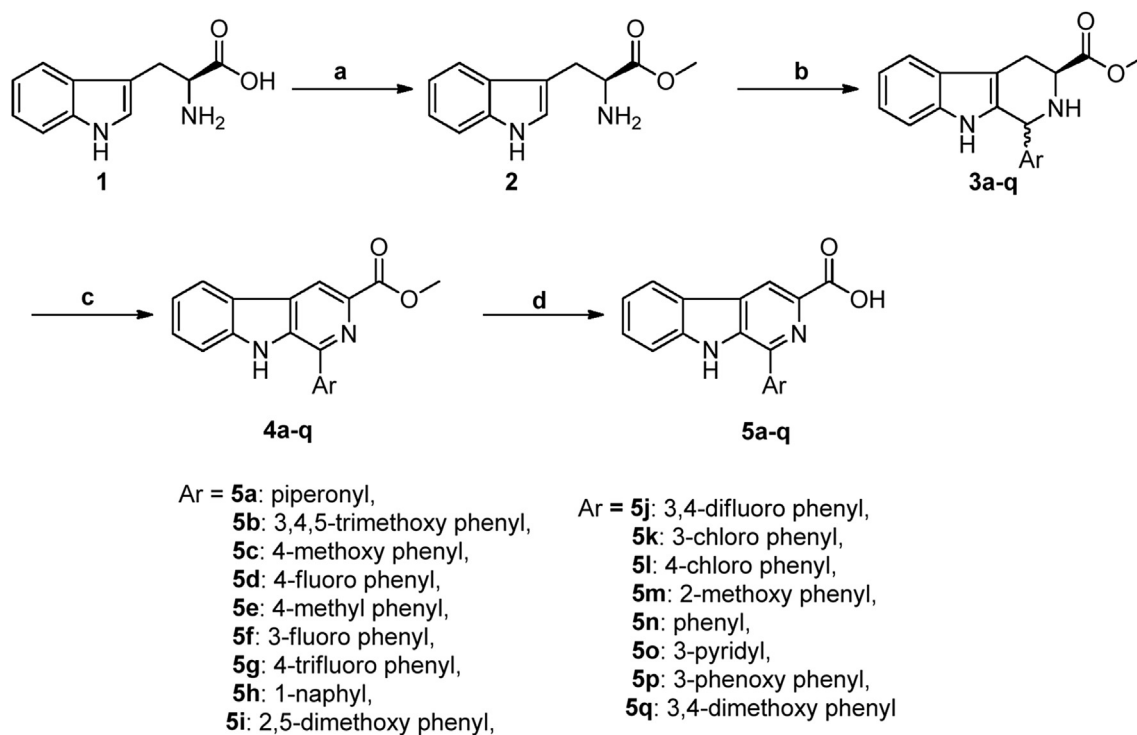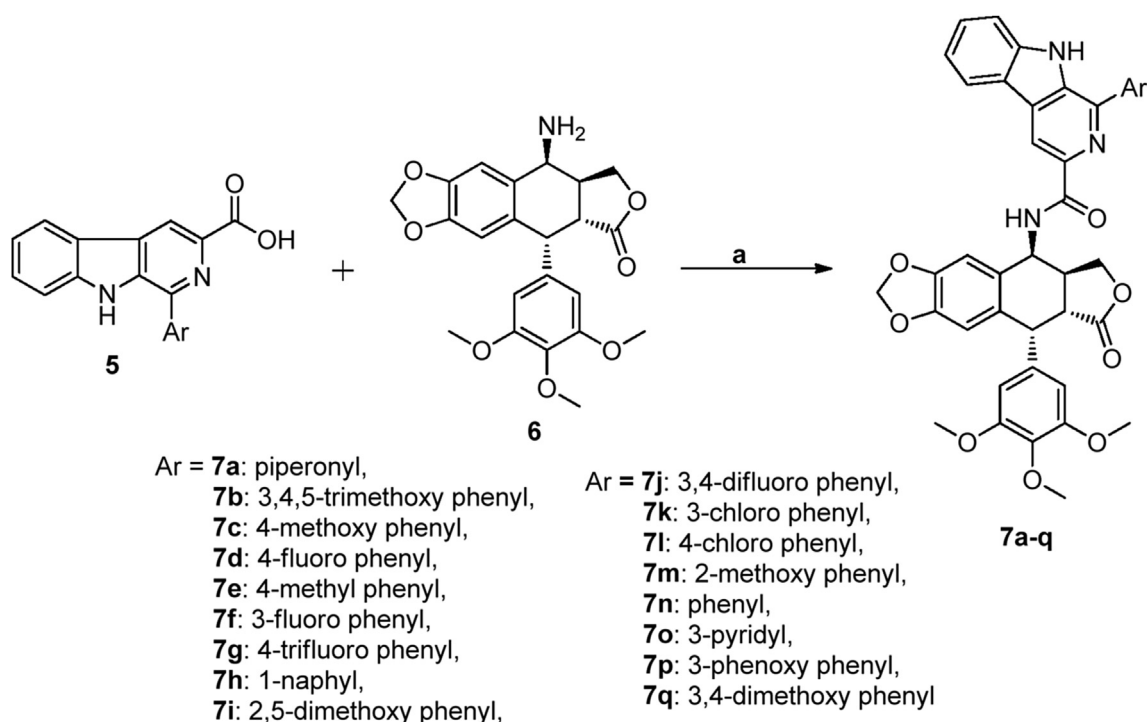


**Fig. 2.** The strategy of target molecules design.

Ar = **5a**: piperonyl,
　　**5b**: 3,4,5-trimethoxy phenyl,
　　**5c**: 4-methoxy phenyl,
　　**5d**: 4-fluoro phenyl,
　　**5e**: 4-methyl phenyl,
　　**5f**: 3-fluoro phenyl,
　　**5g**: 4-trifluoro phenyl,
　　**5h**: 1-naphyl,
　　**5i**: 2,5-dimethoxy phenyl,

Ar **= 5j**: 3,4-difluoro phenyl,
　　**5k**: 3-chloro phenyl,
　　**5l**: 4-chloro phenyl,
　　**5m**: 2-methoxy phenyl,
　　**5n**: phenyl,
　　**5o**: 3-pyridyl,
　　**5p**: 3-phenoxy phenyl,
　　**5q**: 3,4-dimethoxy phenyl

**Scheme 1.** a) SOCl$_2$, MeOH, 0 °C–rt, 12 h, 90%; b) substituted benzaldehyde, *p*-TSA, EtOH, reflux, 12 h; c) TCICA, Et$_3$N, DMF, 0 °C–rt, 2 h, 70–95%; d) NaOH, MeOH, water, reflux, 6 h, 50–70%.



Ar = **7a**: piperonyl,
　　**7b**: 3,4,5-trimethoxy phenyl,
　　**7c**: 4-methoxy phenyl,
　　**7d**: 4-fluoro phenyl,
　　**7e**: 4-methyl phenyl,
　　**7f**: 3-fluoro phenyl,
　　**7g**: 4-trifluoro phenyl,
　　**7h**: 1-naphyl,
　　**7i**: 2,5-dimethoxy phenyl,

Ar = **7j**: 3,4-difluoro phenyl,
　　**7k**: 3-chloro phenyl,
　　**7l**: 4-chloro phenyl,
　　**7m**: 2-methoxy phenyl,
　　**7n**: phenyl,
　　**7o**: 3-pyridyl,
　　**7p**: 3-phenoxy phenyl,
　　**7q**: 3,4-dimethoxy phenyl

**Scheme 2.** a) EDCI, HOBt, DIPEA, CH$_2$Cl$_2$, rt, 12 h, 80–90%.

single-strand DNA breaks, double-strand DNA breaks on treating the DU-145 cells with **7i** and **7j** comparing with etoposide. In the present assay propidium iodide, a fluorescent DNA-binding molecule is used to detect the extent of DNA damage. DU-145 cells were treated with 10 μM of **7i**, **7j** and etoposide, and after lysis the samples were allowed to undergo electrophoresis. Cells grown in the absence of any congeners is considered as control. It was observed that the DNA damage in presence of **7i**, **7j** and etoposide. However, there is no DNA damage observed in the control. Etoposide is well known topoisomerase II inhibitor which exhibits this

**Table 1**
The effect of β-carboline-podophyllotoxin congeners **7a–q** on half maximum inhibitory concentration (IC$_{50}$ values expressed in μM)[a] against a panel of human cancer cell lines.

| Compound | A549[b] | DU-145[c] | MDA MB-231[d] | HT-29[e] | Hela[f] | HEK-293[g] |
|---|---|---|---|---|---|---|
| **7a** | 21.78 ± 1.31 | 14.49 ± 0.09 | 34.28 ± 0.56 | 30.59 ± 2.54 | 15.31 ± 0.25 | 70.60 ± 1.18 |
| **7b** | 103.86 ± 0.28 | 40.29 ± 1.97 | 58.75 ± 1.55 | 86.47 ± 1.60 | 72.93 ± 5.02 | 167.53 ± 0.30 |
| **7c** | 29.44 ± 3.09 | 16.78 ± 0.15 | 33.97 ± 0.82 | 35.65 ± 5.89 | 21.87 ± 1.50 | 65.02 ± 0.36 |
| **7d** | 10.21 ± 0.95 | 5.07 ± 0.97 | 10.72 ± 0.35 | 11.49 ± 0.40 | 15.54 ± 2.95 | 109.07 ± 2.79 |
| **7e** | 16.75 ± 2.76 | 8.74 ± 1.13 | 16.39 ± 1.97 | 19.96 ± 4.47 | 9.77 ± 2.06 | 59.36 ± 0.17 |
| **7f** | 36.37 ± 2.32 | 48.42 ± 0.78 | 80.36 ± 1.31 | 55.70 ± 0.28 | 26.54 ± 0.96 | 104.00 ± 1.78 |
| **7g** | 34.12 ± 0.17 | 24.78 ± 1.29 | 75.94 ± 4.94 | 46.52 ± 6.04 | 32.09 ± 2.32 | 63.04 ± 1.63 |
| **7h** | 56.92 ± 2.78 | 22.02 ± 3.57 | 27.85 ± 1.49 | 22.96 ± 3.52 | 33.02 ± 2.51 | 77.34 ± 0.12 |
| **7i** | **1.87 ± 0.51** | **1.07 ± 0.07** | **2.64 ± 1.17** | **2.68 ± 1.71** | **2.92 ± 1.12** | **103.28 ± 2.43** |
| **7j** | **2.24 ± 0.22** | **1.14 ± 0.16** | **2.90 ± 1.41** | **3.53 ± 0.52** | **3.72 ± 0.37** | **105.94 ± 2.86** |
| **7k** | 3.16 ± 0.66 | 2.41 ± 1.37 | 3.29 ± 0.48 | 5.26 ± 0.52 | 6.09 ± 0.10 | 130.85 ± 0.21 |
| **9l** | 3.98 ± 0.25 | 2.65 ± 0.93 | 3.87 ± 1.00 | 5.77 ± 0.56 | 6.61 ± 0.22 | 58.86 ± 3.11 |
| **7m** | 1.94 ± 0.98 | 1.41 ± 0.54 | 2.69 ± 0.42 | 4.30 ± 0.52 | 4.12 ± 0.20 | 107.20 ± 0.57 |
| **7n** | 2.00 ± 1.34 | 1.68 ± 0.71 | 2.60 ± 0.13 | 6.87 ± 2.11 | 5.26 ± 0.52 | 75.02 ± 2.01 |
| **7o** | 2.55 ± 0.29 | 1.98 ± 0.58 | 3.05 ± 0.06 | 6.36 ± 0.08 | 4.72 ± 0.06 | 84.33 ± 7.55 |
| **7p** | 5.19 ± 0.42 | 3.17 ± 1.54 | 7.52 ± 0.86 | 10.33 ± 0.78 | 11.24 ± 1.75 | 101.56 ± 5.43 |
| **7q** | 12.67 ± 0.95 | 9.16 ± 3.61 | 15.49 ± 0.50 | 14.30 ± 0.10 | 13.38 ± 1.13 | 89.82 ± 1.90 |
| **Doxorubicin** | 1.68 ± 0.93 | 1.86 ± 1.17 | 1.32 ± 0.32 | 1.41 ± 0.04 | 1.91 ± 0.19 | ND |
| **Etoposide** | 2.27 ± 0.11 | 1.97 ± 0.45 | 1.91 ± 0.84 | 1.64 ± 0.50 | 1.93 ± 0.82 | ND |
| **Podophyllotoxin** | 3.76 ± 0.31 | 3.11 ± 0.85 | 9.76 ± 0.31 | 2.99 ± 0.24 | 3.04 ± 1.20 | ND |

ND: Not determined.
The bolded IC50 values are least values (more active) within the cell lines.
 [a] 50% Inhibitory concentration after 48 h of drug treatment and the values are average of three individual experiments.
 [b] Lung cancer.
 [c] Prostate cancer.
 [d] Breast cancer.
 [e] Colon cancer.
 [f] Cervical cancer.
 [g] Normal cells.
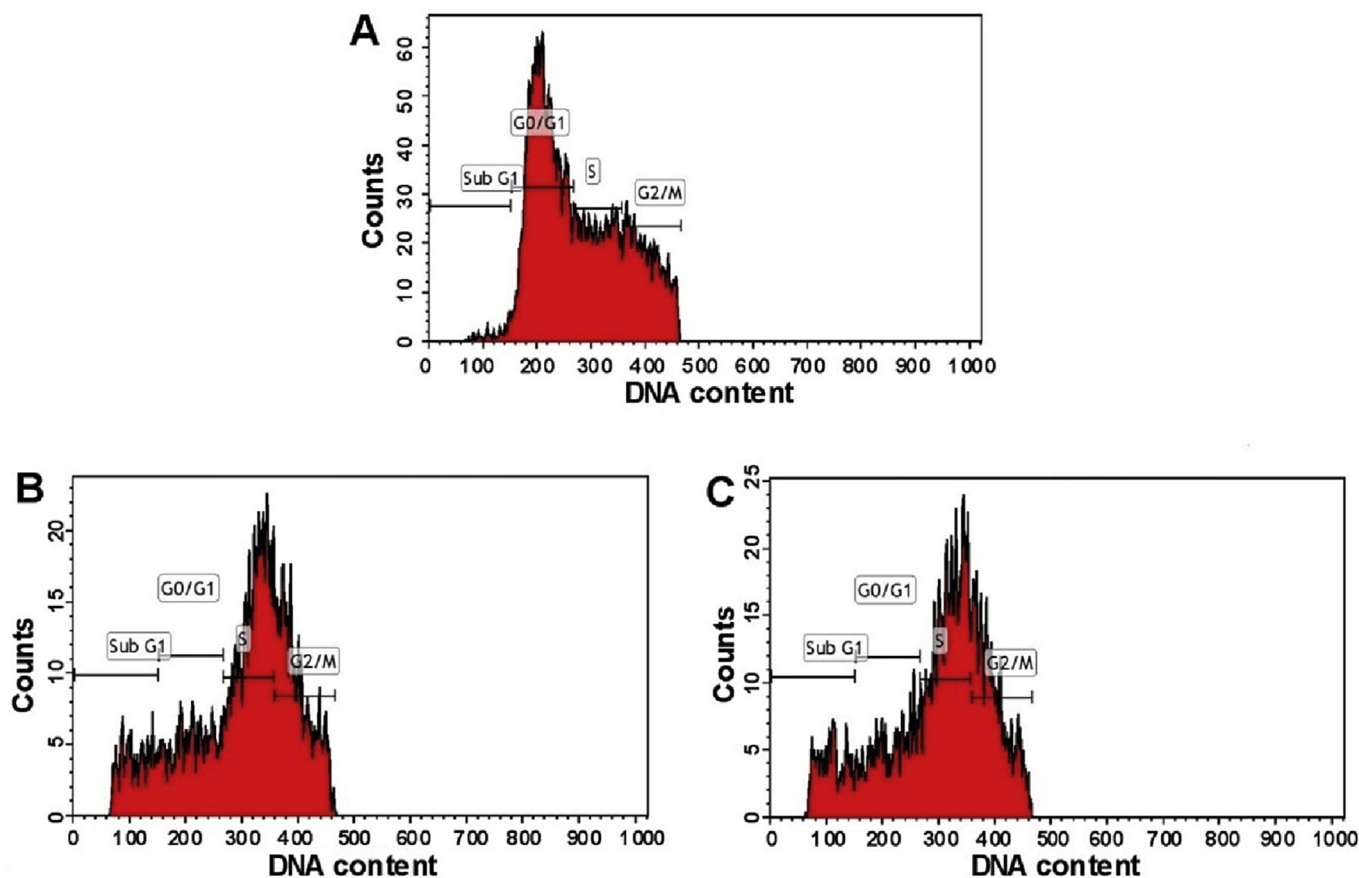


**Fig. 3.** Flow cytometric analysis in DU-145 cell lines after treatment congeners **7i** and **7j** with 1.0 μM concentrations each for 48 h; (A) control cells (DU-145); (B) **7i** (1.0 μM) and (C) **7j** (1.0 μM).

**Table 2**
Cell cycle results observed on treatment of DU-145 cells with 1.0 μM concentration of **7i** and **7j**.

| Sample | Sub $G_1$ (%) | $G_0/G_1$ (%) | S (%) | $G_2$/M (%) |
|---|---|---|---|---|
| control | 1.49 | 51.28 | 24.99 | 21.71 |
| **7i** | 10.79 | 18.69 | 41.44 | 29.16 |
| **7j** | 10.90 | 18.41 | 39.65 | 28.08 |

inhibition activity through stabilizing the DNA cleavable complex. It was reported earlier that etoposide will induce the formation of open circular and linear DNA through the topoisomerase-DNA cleavable complex formation [27b]. We speculate that **7i** and **7j** can also effectively damage the DNA like etoposide and inhibit the activity of topoisomerase II. From Fig. 5, it is clear that the congeners **7i** and **7j** are efficient in damaging the DNA equally.

### 2.2.5. DNA binding studies

To find out the nature of interaction of active congeners **7i** and **7j** with DNA, biophysical studies such as UV−visible spectroscopy, fluorescence spectroscopy and circular dichroism spectroscopy were carried out.

#### 2.2.5.1. UV−visible spectroscopy.
In order to examine the binding nature of active congeners **7i** and **7j** to DNA, the UV absorption spectra of these congeners in the presence and absence of increasing concentrations of CT-DNA were examined (Fig. 6). On addition of equal alliquots of CT-DNA to the solution of these congeners (**7i** and **7j**), absorption band at around 207 nm which gradually decreased without any shift with incresing concentration of CT-DNA was observed. From UV−visible titration data, the **7i** and **7j** congeners with CT-DNA binding constatnts were found to be in the range of $\approx 1 \times 10^4\,M^{-1}$. Since the absorption band at 207 nm shows hyperchromicity upon addition of DNA, it is evident that these congeners could bind to the surface of DNA [28]. The hyperchromic effect may also be due to the electrostatic interaction between **7i** and **7j** and the phosphates in the backbone at the periphery of the double helix CT-DNA [29]. However, it is not possible to understand the binding nature of congeners with UV−visible titration data alone. The representative UV−visible spectra obtained on interaction of complex with CT-DNA is shown in Fig. 6.

#### 2.2.5.2. Fluorescence spectroscopy.
Fluorescence titration is another helpful technique for understanding the binding mode of small molecules with DNA and to study the electronic environment around the DNA-complex at relatively lower concentrations [30]. As these congeners show fluorescence properties, their interaction with CT-DNA could provide certain information about the nature of
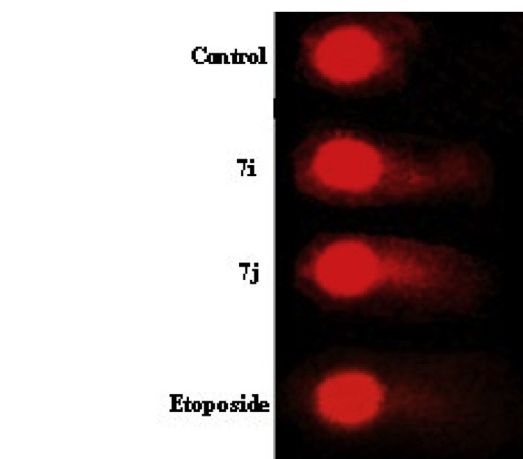
**Fig. 5.** Comet assay: Control; **7i** (10 μM); **7j** (10 μM); etoposide.

their interactions with DNA. In this study, **7i** and **7j** emission spectra show a prominent peak at 409 nm and small humps at 325 nm and 335 nm and on addition of equal increments of CT-DNA solution to the solution of **7i** and **7j**, the hypochromicity of fluorescence emission intensity at 409 was observed, which probably indicates non-intercalative mode of binding such as electrostatic binding mode (surface binding or grove binding) that leads to effective protection of **7i** and **7j** molecules by DNA. However, the less intense fluorescence peaks intensity at 325 and 335 nm exhibited gradual enhancement with the addition of CT-DNA. The enhancement in the fluorescence peaks at lower wavelength may be due to partial intercalating portion of **7i** and **7j** with DNA. But the prominent fluorescence emission at 409 nm clearly showed a gradual reduction in its intensity. Sometimes, the fluorescence emission band hypochromicity may also be due to the quenching of fluorescence emission by surrounding water molecules by absorbing the fluorescence emission energy. The fluorescence spectra of **7i** and **7j** were shown in Fig. 7.

#### 2.2.5.3. Circular dichroism spectroscopy.
In order to study the effect of active congeners **7i** and **7j** on DNA conformation, circular dichoism (CD) studies were performed. The CD spectra of CT-DNA exhibited positive and negative bands at 275 nm and 245 nm respectively. In this study, at an average both the congeners **7i** and **7j** demonstrated around 5−7% hypochromicity of positive CD band on treatment of CT-DNA. On addition of 10 μM of **7i** and **7j** to CT-DNA (1:1 ratio of congener:CT DNA), the positive CD band showed hypochromicity which indicates that unwinding of CT-DNA
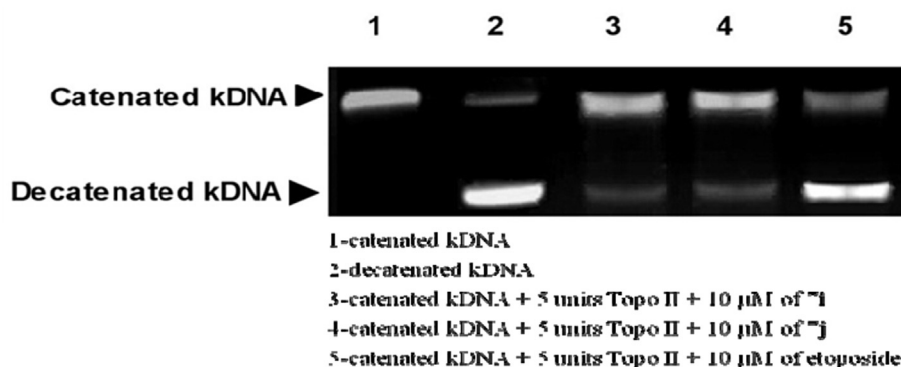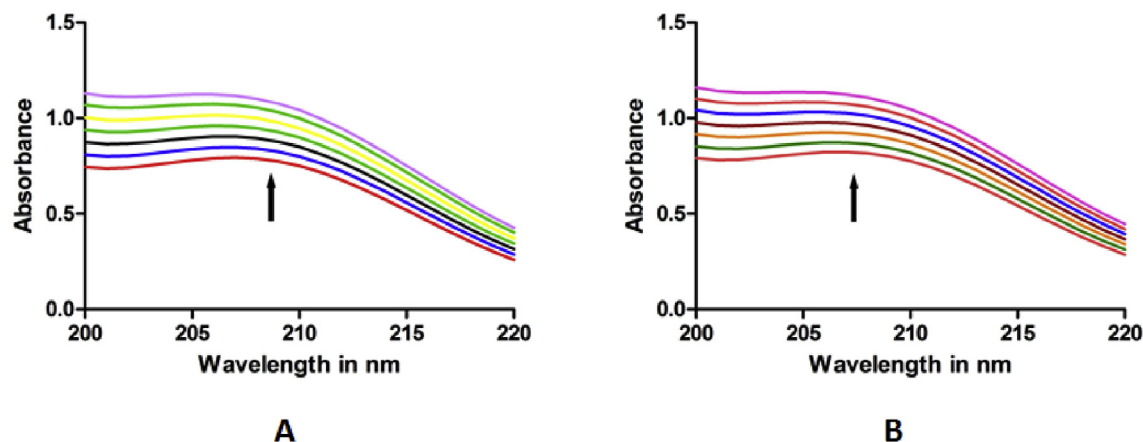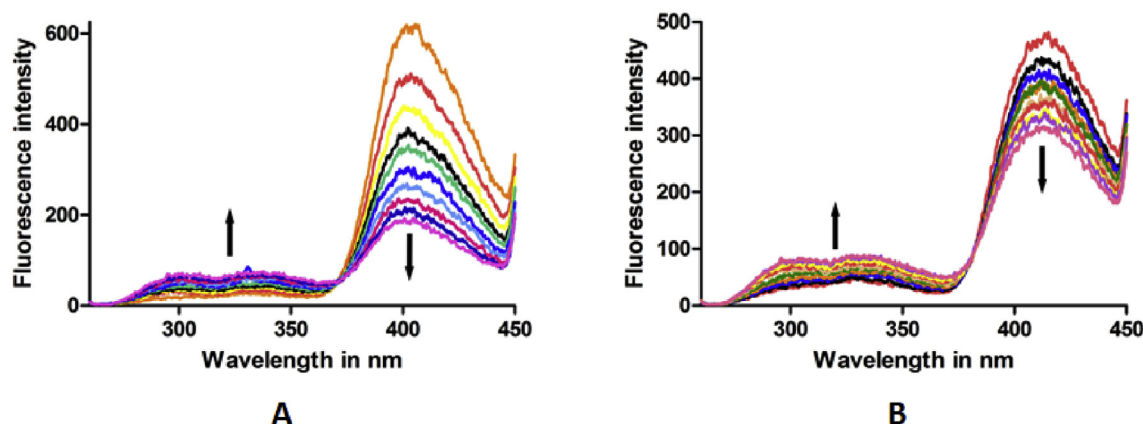
1-catenated kDNA
2-decatenated kDNA
3-catenated kDNA + 5 units Topo II + 10 μM of **7i**
4-catenated kDNA + 5 units Topo II + 10 μM of **7j**
5-catenated kDNA + 5 units Topo II + 10 μM of etoposide

**Fig. 4.** DNA topo II inhibition assay of **7i** and **7j**.

**Fig. 6.** UV−visible spectroscopy of **7i** and **7j** with CT-DNA.



**Fig. 7.** Fluorescence spectroscopy of **7i** and **7j** with CT-DNA.

due to the interaction of **7i** and **7j** with CT-DNA [31]. Next, on doubling the concentration of congeners (20 μM **7i/7j**:10 μM CT DNA), the positive band intensity was further reduced. Based on these observations, CD studies indicates that **7i** and **7j** would interact with DNA and bring small changes in DNA conformation. The CD spectra of **7i** and **7j** with CT-DNA is shown in Fig. 8.

### 2.3. Molecular docking studies

To visualize the binding mode of the title compounds, molecular docking studies were performed with ATP-binding domain of human topoisomerase-IIα. The results of the docking study are in correlation with the DNA topoisomerase-IIα inhibition assay in which, the synthesized compounds occupied the ATP-binding active site with similar orientations and formed strong interactions with several surrounding residues. Fig. 9 represents the docking pose of **7i** and **7j** in the ATP binding pocket, where it is enclosed by Asn91, Asn95, Arg98, Gly124, Ile125, Pro126, Ile141, Gly164, and Gly166 residues. The lactone oxygen of podophyllotoxin ring system forms hydrogen-bonding with the side chain of
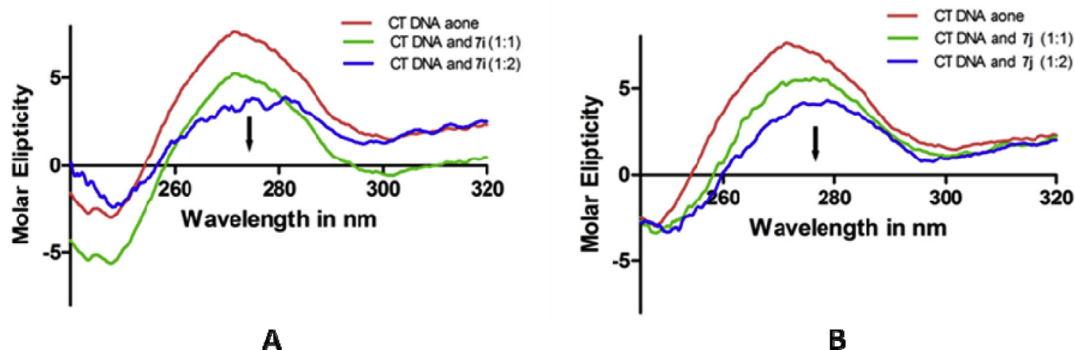


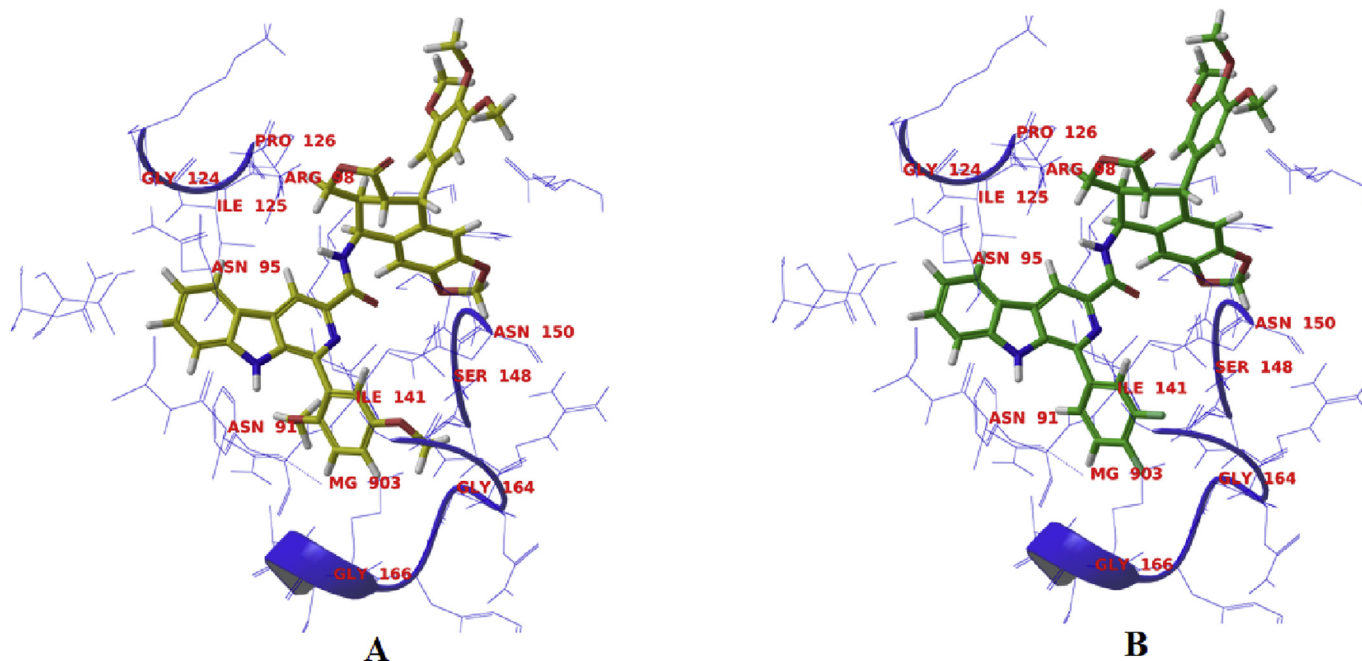**Fig. 8.** Circular dichroism spectroscopy of **7i** and **7j** with CT-DNA.

**Fig. 9.** View of compound **7i** (**A**) and **7j** (**B**) docked in the ATP binding domain of human topoisomerase IIα.

Arg 98. Additionally, the methoxy group in **7i** and fluorine in **7j** on the C-1 phenyl of β-carboline ring form hydrogen-bonding with the side chain of Asn150. Further, the entry of ATP into the binding site is also hindered by the interactions of the compounds with the $Mg^{+2}$ ion and residues below the ATP binding site (Asn46, Asp73, Ile78, Arg136 and Tyr165).

Molecular docking simulations were also carried out into the DNA duplex d(CGCGAATTCGCG)₂. The docked poses for top scored **7i** and **7j**, shown in Fig. 10, depict the ability of the amide functionality to orient the molecules perfectly in a curved shape along length of the minor groove. Further, the docked poses were stabilized by hydrogen bonding between the indole NH-, amide group and the side chains of the DNA base pairs. The aromatic ring in the β-carboline as well as the podophyllotoxin parts were also observed to be involved in side wise $\pi-\pi$ stacking with the base pairs. All these interactions strengthen the minor groove binding affinity of the β-carboline-linked podophyllotoxin derivatives. These results are in agreement with the DNA binding studies as well as the cytotoxicity data.

## 3. Conclusion

In conclusion, we have synthesized a series of new β-carboline-podophyllotoxin congeners by amidation of different β-carboline acids with 4β-aminopodophyllotoxin. The target congeners contain two well established pharmacophoric groups such as β-carboline ring system, podophyllotoxin and the congeners **7i** and **7j** found to be most active in the series. Further, these assayed for cell cycle analysis and DNA topo II inhibitory activity using catenated kDNA. However, these studies revealed that the **7i** and **7j** inhibit efficiently topo II enzymatic activity by catalytic inhibition of topo II. The DNA binding studies disclosed that **7i** and **7j** are DNA external binders and the docking studies correlated with DNA binding studies as well as topo II inhibition studies. Overall, these studies are very important to understand the role of different pharmacophores that are connected to β-carboline nucleus or podophyllotoxin nucleus for the cytotoxic activity, DNA binding ability and DNA topo II inhibitory activity.

## 4. Experimental section

### 4.1. Materials and methods

Chemical reagents were purchased from Sigma-Aldrich and used without further purification. All the solvents were of commercial grade and were purified prior to use when necessary. ¹H and ¹³C NMR experiments were performed on Avance (300 MHz, 400 MHz and 500 MHz) spectrometers. Chemical shifts are measured relative to an internal standard tetramethylilane (TM) set to $\delta$ 0 ppm and are reported in parts per million (ppm). Spin multiplicities are described as s (singlet), br s (broad singlet), d (doublet), dd (double doublet), t (triplet), td (triple doublet), q (quartet), or m (multiplet). Coupling constants are reported in hertz (Hz). TLC analyses were performed with silica gel plates (0.25 mm, E. Merck, 60 F254) using iodine, KMnO4, and a UV lamp for visualization. Specific rotations were measured on a Perkin-Elmer 341MC polarimeter. Mass spectra were recorded by electrospray ionization mass spectrometry (ESI-MS). HRMS was performed on a Varian QFT-ESI instrument. Melting points were determined on an electrothermal melting point apparatus and are uncorrected. IR spectra were measured on Bruker FT-IR Equinox 55 and Bruker TENSOR 27 instruments.

### 4.2. Preparation of (S)-methyl 2-amino-3-(1H-indol-3-yl) propanoate (2) [32]

To the stirred solution of L-tryptophan (**1**, 1 mmol) in methanol (50 ml), thionyl chloride (8.02 mL, 1.1 mol) was added drop-wise at 0 °C and continued stirring for 12 h at room temperature. The excess amount of solvent was removed under vacuum and dried well. Then, the resulting solid was dissolved in CH₂Cl₂, basified with saturated NaHCO₃ solution and extracted with excess amount of CH₂Cl₂. Then, the organic layer was dried over anhydrous Na₂SO₄ and concentrated *in vacuo* to obtain L-tryptophan methyl ester (**2**). White solid; 19.62 g; 90% yield; Mp: 102–103 °C; ¹H NMR (300 MHz, CDCl₃) $\delta$ (ppm) 8.81 (bs, 1H), 7.58 (d, $J$ = 7.90 Hz, 1H), 7.25 (d, $J$ = 7.90 Hz, 1H), 7.14 (t, $J$ = 6.90, 7.14 Hz, 1H), 7.08 (t, $J$ = 6.90,
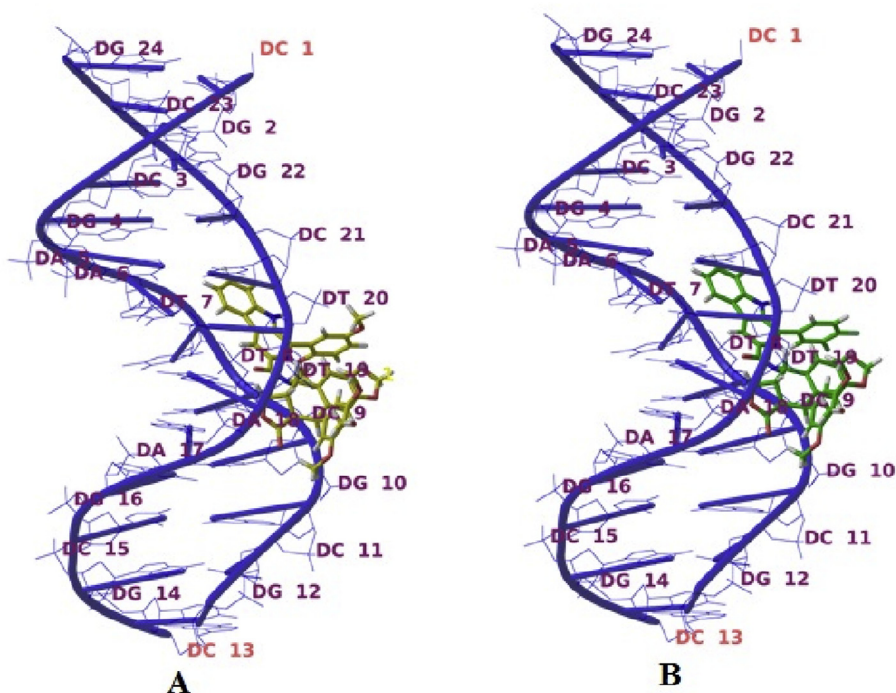
**Fig. 10.** Binding poses of **7i** (**A**) and **7j** (**B**) in the minor groove of d(CGCGAATTCGCG)₂.

7.14 Hz, 1H), 6.90 (s, 1H), 3.84 (t, *J* = 4.90, 5.42 Hz, 1H), 3.73 (s, 3H), 3.25 (dd, *J* = 4.45, 13.8 Hz, 1H), 3.00 (dd, *J* = 4.12, 13.8 Hz, 1H), 2.00 (s, 2H); ESI-MS: *m/z* 219 [M+H] ⁺.

### 4.3. General reaction procedure for the preparation of compounds 4a–q

To a mixture of ʟ–tryptophan ester (**2**, 1 mmol) and substituted benzaldeyde (1.1 mmol) in EtOH, added catalytic *p*-TSA and refluxed for 12 h. After completion of the reaction, solvent was removed *in vacuo* and the crude product **3a–c** (1.0 mmol) was taken in DMF and treated with TEA (3.0 mmol), a solution of TCICA (1.1 mmol) in DMF was added dropwise at −20 °C. The reaction mixture was allowed slowly to 0 °C and stirred at same temperature for 2 h. After the completion of reaction, reaction mixture was quenched with ice water. The precipitate was filtered, washed with water, and dried *in vacuo* to give the compound (**4a–q**).

#### 4.3.1. Methyl 1-(benzo[d][1,3]dioxol-5-yl)-9H-pyrido[3,4-b]indole-3-carboxylate (4a) [33a]

White solid; 92% yield; mp: 292–294 °C; ¹H NMR (300 MHz, DMSO–*d₆*) δ (ppm): 8.89 (s, 1H), 8.42 (d, *J* = 7.9 Hz, 1H), 7.70 (d, *J* = 8.3 Hz, 1H), 7.61 (d, *J* = 7.1 Hz, 0.9H), 7.58–7.51 (m, 2H), 7.32 (t, *J* = 7.1 Hz, 1H), 7.18 (d, *J* = 8.3 Hz, 0.9H), 6.17 (s, 1.8H), 3.93 (s, 3H) the extra peaks at 7.45, 7.10, 6.14 are due to 10% minor rotamer; ESI-MS: *m/z* 347 [M+H]⁺.

#### 4.3.2. Methyl 1-(3,4,5-trimethoxyphenyl)-9H-pyrido[3,4-b]indole-3-carboxylate (4b) [23a,33]

Yellow solid: 80% yield; mp: 229–230 °C; ¹H NMR (300 MHz, CDCl₃) δ (ppm): 9.38 (bs, 1H), 8.75 (s, 1H), 8.21(d, *J* = 7.5 Hz, 1H), 7.60 (d, *J* = 7.5 Hz, 1H), 7.56–7.61 (m, 1H), 7.32–7.38 (m, 1H), 6.94 (s, 2H), 4.03 (s, 3H), 3.84 (s, 3H), 3.77 (s, 6H); ESI-MS: *m/z* 393 [M+H]⁺.

#### 4.3.3. Methyl 1-(4-methoxyphenyl)-9H-pyrido[3,4-b]indole-3-carboxylate (4c) [23,33a]

White solid; 95% yield; mp: 226–230 °C; ¹H NMR (300 MHz, CDCl₃) δ (ppm): 9.18 (bs, 1H), 8.80 (s, 1H), 8.17 (d, *J* = 7.7 Hz, 1H), 7.78 (d, *J* = 8.8 Hz, 2H), 7.57–7.55 (m, 2H), 7.36–7.33 (m, 1H), 6.88 (d, *J* = 8.6 Hz, 2H), 4.03 (s, 3H), 3.77 (s, 3H); ESI-MS: *m/z* 333 [M+H]⁺.

#### 4.3.4. Methyl 1-(4-fluorophenyl)-9H-pyrido[3,4-b]indole-3-carboxylate (4d) [23a,33a]

White solid: 73% yield; mp: 195–198 °C; ¹H NMR (500 MHz, CDCl₃) δ (ppm): 4.06 (s, 3H), 7.22 (t, *J* = 8.7 Hz, 2H), 7.39 (t, *J* = 7.9 Hz, 1H), 7.63–7.55 (m, 2H), 7.92 (q, *J* = 5.3, 8.7 Hz, 2H), 8.22 (d, *J* = 7.8 Hz, 1H), 8.83 (bs, 1H), 8.87 (s, 1H); ESI-MS: *m/z* 321 [M+H]⁺.

#### 4.3.5. Methyl 1-(p-tolyl)-9H-pyrido[3,4-b]indole-3-carboxylate (4e) [33a]

Yellow solid: 90% yield; mp: 192–194 °C; ¹H NMR (500 MHz, DMSO–*d₆*) δ (ppm): 8.90 (s, 1H), 8.42 (d, *J* = 7.8 Hz, 1H), 7.93 (d, *J* = 9.1 Hz, 2H), 7.70 (d, *J* = 8.2 Hz, 1H), 7.60 (t, *J* = 8.2 Hz, 1H), 7.45 (d, *J* = 7.9 Hz, 2H), 7.32 (t, *J* = 7.9 Hz, 1H), 3.93 (s, 3H), 2.45 (s, 3H); ESI-MS: *m/z* 317 [M+H]⁺.

#### 4.3.6. Methyl 1-(3-fluorophenyl)-9H-pyrido[3,4-b]indole-3-carboxylate (4f) [33a]

Light yellow solid: 75% yield; mp: 224–228 °C; ¹H NMR (300 MHz, CDCl₃) δ (ppm): 11.16 (s, 1H), 8.95 (s, 1H), 8.44 (d, *J* = 7.9 Hz, 1H), 7.91–7.84 (m, 1H), 7.83–7.77 (m, 1H), 7.73–7.67 (m, 2H), 7.66–7.59 (m, 1H), 7.46–7.31 (m, 2H), 3.94 (s, 3H); ESI-MS: *m/z* 321 [M+H]⁺.

#### 4.3.7. Methyl 1-(4-(trifluoromethyl)phenyl)-9H-pyrido[3,4-b]indole-3-carboxylate (4g) [23,33]

Pale yellow solid; 79% yield; mp: 250–252 °C; ¹H NMR (300 MHz, DMSO–*d₆*) δ (ppm): 3.94 (s, 3H), 7.32 (t, *J* = 7.5 Hz, 1H),

7.59 (t, *J* = 7.9 Hz, 1H), 7.68 (d, *J* = 8.1 Hz, 1H), 7.92 (d, *J* = 8.1 Hz, 2H), 8.23 (d, *J* = 7.7 Hz, 2H), 8.36 (d, *J* = 7.7 Hz, 1H), 8.93 (s, 1H), 11.99 (bs, 1H); ESI-MS: *m/z* 371 [M+H]⁺.

### 4.3.8. Methyl 1-(naphthalen-1-yl)-9H-pyrido[3,4-b]indole-3-carboxylate (4h) [33b]

White solid: 95% yield; mp: 294–297 °C; ¹H NMR (300 MHz, DMSO–*d*₆) δ (ppm): 11.61 (s, 1H), 9.05 (s, 1H), 8.48 (d, *J* = 7.7 Hz, 1H), 8.16 (dd, *J* = 2.5, 6.8 Hz, 1H), 8.11 (d, *J* = 8.1 Hz, 1H), 7.78–7.73 (m, 2H), 7.62–7.53 (m, 4H), 7.44 (t, *J* = 6.9 Hz, 1H), 7.33 (t, *J* = 7.7 Hz, 1H), 3.90 (s, 3H); ESI-MS: *m/z* 353 [M+H]⁺.

### 4.3.9. Methyl 1-(2,5-dimethoxyphenyl)-9H-pyrido[3,4-b]indole-3-carboxylate (4i)

Creamish solid; 80% yield; mp: 290–294 °C; ¹H NMR (300 MHz, DMSO–*d*₆) δ (ppm): 11.51 (s, 1H), 8.92 (s, 1H), 8.40 (d, *J* = 8.3 Hz, 1H), 7.64–7.55 (m, 2H), 7.30 (t, *J* = 6.8 Hz, 1H), 7.22–7.11 (m, 2H), 7.04 (d, *J* = 1 Hz), 3.91 (s, 3H), 3.77 (s, 3H), 3.69 (s, 3H); ESI-MS: *m/z* 363 [M+H]⁺.

### 4.3.10. Methyl 1-(3,4-difluorophenyl)-9H-pyrido[3,4-b]indole-3-carboxylate (4j) [34]

Off-white solid; 78% yield; mp: 236–239 °C; ¹H NMR (300 MHz, DMSO–*d*₆) δ (ppm): 3.94 (s, 3 H), 7.32–7.37 (m, 1 H), 7.42–7.49 (m, 1 H), 7.60–7.78 (m, 4 H), 8.46 (d, *J* = 7.93 Hz, 1 H), 8.97 (s, 1H), 12.05 (bs, 1H); ESI-MS: *m/z* 339 [M+H]⁺.

### 4.3.11. Methyl 1-(3-chlorophenyl)-9H-pyrido[3,4-b]indole-3-carboxylate (4k) [34]

Pale yellow solid; 80% yield; mp: 209–211 °C; ¹H NMR (300 MHz, DMSO–*d*₆) δ (ppm): 3.94 (s, 3H), 7.27–7.32 (m, 1 H), 7.47–7.71 (m, 4H), 7.98 (d, *J* = 10.38 Hz, 2H), 8.31 (s, 1 H), 8.87 (s, 1 H), 11.93 (bs, 1H); ESI-MS: *m/z* 337 [M+H]⁺.

### 4.3.12. Methyl 1-(4-chlorophenyl)-9H-pyrido[3,4-b]indole-3-carboxylate (4l) [33b]

Yellow solid: 93% yield; mp: 268–272 °C; ¹H NMR (300 MHz, CDCl₃ + DMSO–*d*₆) δ (ppm): 8.81 (s, 1H), 8.23 (d, *J* = 7.7 Hz, 1H), 8.01 (d, *J* = 8.3 Hz, 1H), 7.64 (d, *J* = 8.3 Hz, 1H), 7.59–7.51 (m, 3H), 7.27 (t, *J* = 7.2 Hz, 1H), 6.92 (d, *J* = 7.4 Hz, 1H), 3.93 (s, 3H); ESI-MS: *m/z* 337 [M+H]⁺.

### 4.3.13. Methyl 1-(2-methoxyphenyl)-9H-pyrido[3,4-b]indole-3-carboxylate (4m) [33a]

White solid; 88% yield; mp: 208–210 °C; ¹H NMR (500 MHz, CDCl₃) δ (ppm): 8.91 (d, *J* = 0.4 Hz, 1H), 8.75 (bs, 1H), 8.22 (d, *J* = 7.9 Hz, 1H), 7.79 (dd, *J* = 1.8, 7.6 Hz, 1H), 7.60–7.56 (m, 1H), 7.53 (d, *J* = 8.1 Hz, 1H), 7.50–7.46 (m, 1H), 7.37–7.34 (m, 1H), 7.20–7.17 (m, 1H), 7.12 (d, *J* = 7.6 Hz, 1H), 4.05 (s, 3H), 3.84 (s, 3H); ESI-MS: *m/z* 333 [M+H]⁺.

### 4.3.14. Methyl 1-phenyl-9H-pyrido[3,4-b]indole-3-carboxylate (4n) [33a]

White solid: 88% yield; mp: 257–259 °C; ¹H NMR (300 MHz, DMSO–*d*₆) δ (ppm): 8.92 (s, 1H), 8.42 (d, *J* = 7.9 Hz, 1H), 8.02 (d, *J* = 7.0 Hz, 2H), 7.73–7.54 (m, 5H), 7.33 (t, *J* = 7.7 Hz, 1H), 3.93 (s, 3H); ESI-MS: *m/z* 303 [M+H]⁺.

### 4.3.15. Methyl 1-(pyridin-3-yl)-9H-pyrido[3,4-b]indole-3-carboxylate (4°) [33a]

White solid: 90% yield; mp: 233–236 °C; ¹H NMR (300 MHz, DMSO–*d*₆) δ (ppm): 9.21 (s, 1H), 8.98 (s, 1H), 8.77 (d, *J* = 3.8 Hz, 1H), 8.46 (d, *J* = 7.9 Hz, 1H), 8.42–8.36 (m, 1H), 7.73–7.60 (m, 3H), 7.35 (t, *J* = 7.7 Hz, 1H), 3.94 (s, 3H); ESI-MS: *m/z* 304 [M+H]⁺.

### 4.3.16. Methyl 1-(3-phenoxyphenyl)-9H-pyrido[3,4-b]indole-3-carboxylate (4p)

Creamish solid; 65% yield; mp: 191–195 °C; ¹H NMR (300 MHz, DMSO–*d*₆) δ (ppm): 11.4 (s, 1H), 8.76 (s, 1H), 8.12 (d, *J* = 7.7 Hz, 1H), 7.73 (d, *J* = 7.7 Hz, 1H), 7.66–7.58 (m, 2H), 7.52–7.44 (m, 2H), 7.30–7.22 (m, 3H), 7.06–6.97 (m, 4H), 3.93 (s, 3H); ESI-MS: *m/z* 395 [M+H]⁺.

### 4.3.17. Methyl 1-(3,4-dimethoxyphenyl)-9H-pyrido[3,4-b]indole-3-carboxylate (4q)

Creamish solid; 82% yield; mp: 198–202 °C; ¹H NMR (300 MHz, DMSO–*d*₆) δ (ppm): 8.83 (s, 1H), 8.35 (d, *J* = 7.7 Hz, 1H), 7.69 (d, *J* = 8.3 Hz, 1H), 7.60 (d, *J* = 7.9 Hz, 1H), 7.57–7.51 (m, 2H), 7.32 (t, *J* = 7.7 Hz, 1H), 7.18 (d, *J* = 8.8 Hz, 1H), 3.91 (s, 3H), 3.87 (s, 3H), 3.85 (s, 3H); ESI-MS: *m/z* 363 [M+H]⁺.

### 4.4. General procedure for the synthesis of compounds 5a–q

To the stirred suspension of compound **4a–q** (1 mmol) in MeOH was added aqueous solution of NaOH (2 mmol) and stirred for 6 h at 70 °C. The solvent was evaporated *in vacuo* and the obtained residue was acidified with 10% citric acid solution and the resulted precipitate was filtered, washed with ethanol and dried. These well dried solid products **5a–q** were employed for directly for next step without any further purification.

### 4.5. General procedure for the synthesis of compounds 7a–q

To a stirred solution of compound **5a–q** (1 mmol) and compound **6** [23c] (1 mmol) in DCM were added EDCI (1.2 mmol), HOBt (1.2 mmol) and TEA (3 mmol) at 0 °C and stirred for 16 h at room temperature. The reaction mixture was quenched with ice cold water and extracted with DCM, the combined organic phases were dried over Na₂SO₄ and concentrated under reduced pressure to get crude products **7a–q** which were purified by silica gel column chromatography by using EtOAc/n-hexane.

### 4.5.1. 1-(Benzo[d][1,3]dioxol-5-yl)-N-((5S,5aS,8aR,9R)-8-oxo-9-(3,4,5-trimethoxyphenyl)-5,5a,6,8,8a,9-hexahydrofuro[3′,4′:6,7]naphtho[2,3-d][1,3]dioxol-5-yl)-9H-pyrido[3,4-b]indole-3-carboxamide (7a)

White solid; 80% yield; mp: 190–195 °C; [α]²⁵_D: −67.448 (c = 0.14, CHCl₃); ¹H NMR (500 MHz, CDCl₃) δ (ppm): 8.91 (s, 1H), 8.78 (s, 1H), 8.32 (d, *J* = 7.7 Hz, 1H), 8.22 (d, *J* = 7.9 Hz, 1H), 7.61 (t, *J* = 8.0 Hz, 1H), 7.56 (d, *J* = 8.0 Hz, 1H), 7.41–7.36 (m, 2H), 7.34 (d, *J* = 1.5 Hz, 1H), 7.01 (d, *J* = 7.9 Hz, 1H), 6.87 (s, 1H), 6.57 (s, 1H), 6.35 (s, 2H), 6.07 (s, 2H), 5.98 (d, *J* = 3.9 Hz, 2H), 5.54 (dd, *J* = 4.4 Hz, 7.78 Hz, 1H), 4.68 (d, *J* = 4.5 Hz, 1H), 4.54 (dd, *J* = 7.0 Hz, 9.0 Hz, 1H), 3.99 (t, *J* = 9.4 Hz, 1H), 3.82 (s, 3H), 3.77 (s, 6H), 3.15–3.08 (m, 1H), 3.05 (dd, *J* = 4.5, 14.1 Hz, 1H); ¹³C NMR (75 MHz, CDCl₃) δ (ppm): 174.5, 165.8, 152.6, 148.5, 148.3, 147.6, 141.2, 140.7, 139.1, 137.2, 134.9, 132.4, 131.6, 130.4, 129.2, 129.0, 122.1, 122.0, 121.9, 121.1, 113.8, 111.9, 110.1, 109.3, 108.8, 108.7, 108.3, 101.5, 101.3, 69.2, 60.7, 56.2, 48.1, 43.9, 41.9, 37.7; IR (KBr): 3373.72, 2923.96, 2358.96, 1776.87, 1660.26, 1588.36, 1488.58, 1334.81, 1237.33 cm⁻¹; ESI-MS: *m/z* 728 [M+H]⁺; HRMS: *m/z* calcd. for C₄₁H₃₄N₃O₁₀ 728.22442 [M+H]⁺, found 728.22440.

### 4.5.2. N-((5S,5aS,8aR,9R)-8-Oxo-9-(3,4,5-trimethoxyphenyl)-5,5a,6,8,8a,9-hexahydrofuro[3′,4′:6,7]naphtho[2,3-d][1,3]dioxol-5-yl)-1-(3,4,5-trimethoxyphenyl)-9H-pyrido[3,4-b]indole-3-carboxamide (7b)

White solid; 85% yield; mp: 185–190 °C; [α]²⁵_D: −74.560 (c = 0.17, CHCl₃); ¹H NMR (500 MHz, CDCl₃) δ (ppm): 8.91 (s, 1H), 8.85 (bs, 1H), 8.38 (d, *J* = 7.3 Hz, 1H), 8.24 (d, *J* = 7.9 Hz, 1H), 7.66–7.60 (m, 1H), 7.58 (d, *J* = 8.0 Hz, 1H), 7.40 (t, *J* = 6.7 Hz, 1H), 7.04 (s, 2H),

6.90 (s, 1H), 6.57 (s, 1H), 6.35 (s, 2H), 5.95 (dd, $J = 1.0$ Hz, 17.5 Hz, 2H), 5.48 (dd, $J = 4.5$ Hz, 7.17 Hz, 1H), 4.65 (d, $J = 4.7$ Hz, 1H), 4.57 (dd, $J = 7.3$ Hz, 9.15 Hz, 1H), 4.04 (t, $J = 9.4$ Hz, 1H), 3.94 (s, 3H), 3.89 (s, 6H), 3.82 (s, 3H), 3.77 (s, 6H), 3.16–3.08 (m, 1H), 3.04 (dd, $J = 4.8$, 14.3 Hz, 1H); $^{13}$C NMR (75 MHz, CDCl$_3$) $\delta$ (ppm): 174.4, 165.7, 153.6, 152.5, 148.9, 148.1, 147.4, 141.3, 140.8, 138.9, 138.7, 135.1, 134.8, 133.0, 132.4, 130.9, 130.4, 129.3, 129.0, 122.0, 121.1, 113.8, 111.9, 110.0, 109.2, 108.1, 105.5, 101.4, 69.3, 60.8, 60.6, 56.2, 56.1, 48.3, 43.7, 41.8, 37.7; IR (KBr): 3362.11, 2936.86, 2835.20, 2359.43, 1776.56, 1660.92, 1586.48, 1504.75, 1329.00, 1234.02 cm$^{-1}$; ESI-MS: $m/z$ 774 [M+H]$^+$; HRMS: $m/z$ calcd. for C$_{43}$H$_{40}$N$_3$O$_{11}$ 774.26628 [M+H]$^+$, found 774.26640.

### 4.5.3. 1-(4-Methoxyphenyl)-N-((5S,5aS,8aR,9R)-8-oxo-9-(3,4,5-trimethoxyphenyl)-5,5a,6,8,8a,9-hexahydrofuro[3′,4′:6,7]naphtho[2,3-d][1,3]dioxol-5-yl)-9H-pyrido[3,4-b]indole-3-carboxamide (7c)

White solid; 90% yield; mp: 190–195 °C; [α]$^{25}$$_D$: −68.411 ($c$ = 0.10, CHCl$_3$); $^1$H NMR (500 MHz, CDCl$_3$) $\delta$ (ppm): 8.90 (s, 1H), 8.76 (s, 1H), 8.37 (d, $J = 7.9$ Hz, 1H), 8.23 (d, $J = 7.9$ Hz, 1H), 7.83 (d, $J = 8.8$ Hz, 2H), 7.63–7.58 (m, 1H), 7.55 (d, $J = 8.0$ Hz, 1H), 7.42–7.36 (m, 1H), 7.12 (d, $J = 8.6$ Hz, 2H), 6.87 (s, 1H), 6.56 (s, 1H), 6.35 (s, 2H), 5.97 (dd, $J = 1.2$ Hz, 4.73 Hz, 2H), 5.55 (dd, $J = 4.4$ Hz, 7.78 Hz, 1H), 4.66 (d, $J = 4.5$ Hz, 1H), 4.54 (dd, $J = 7.0$ Hz, 9.15 Hz, 1H), 4.00 (t, $J = 9.3$ Hz, 1H), 3.90 (s, 3H), 3.82 (s, 3H), 3.77 (s, 6H), 3.16–3.08 (m, 1H), 3.05 (dd, $J = 4.7$, 17.1 Hz, 1H); $^{13}$C NMR (75 MHz, CDCl$_3$) $\delta$ (ppm): 174.5, 165.8, 160.4, 152.5, 148.3, 147.6, 141.4, 140.6, 139.1, 135.0, 134.9, 132.3, 130.9, 130.2, 129.9, 129.5, 129.2, 128.9, 122.1, 122.0, 121.1, 114.6, 113.6, 111.8, 110.0, 109.3, 108.2, 101.5, 69.2, 60.7, 56.1, 55.4, 48.0, 43.8, 42.0, 37.6; IR (KBr): 3375.23, 2935.01, 2836.43, 2359.73, 1776.14, 1660.14, 1588.75, 1509.74, 1322.33, 1247.07 cm$^{-1}$; ESI-MS: $m/z$ 714 [M+H]$^+$; HRMS: $m/z$ calcd. for C$_{41}$H$_{36}$N$_3$O$_9$ 714.24515 [M+H]$^+$, found 714.24452.

### 4.5.4. 1-(4-Fluorophenyl)-N-((5S,5aS,8aR,9R)-8-oxo-9-(3,4,5-trimethoxyphenyl)-5,5a,6,8,8a,9-hexahydrofuro[3′,4′:6,7]naphtho[2,3-d][1,3]dioxol-5-yl)-9H-pyrido[3,4-b]indole-3-carboxamide (7d)

White solid; 89% yield; mp: 325–330 °C; [α]$^{25}$$_D$: −75.887 ($c$ = 0.13, CHCl$_3$); $^1$H NMR (500 MHz, CDCl$_3$) $\delta$ (ppm): 8.94 (s, 1H), 8.74 (s, 1H) 8.30 (d, $J = 7.9$ Hz, 1H), 8.24 (d, $J = 7.7$ Hz, 1H), 7.87 (dd, $J = 5.3$, 8.6 Hz, 2H), 7.65–7.60 (m, 1H), 7.56 (d, $J = 8.0$ Hz, 1H), 7.40 (t, $J = 7.0$ Hz, 1H), 7.29 (t, $J = 8.6$ Hz, 2H), 6.87 (s, 1H), 6.57 (s, 1H), 6.35 (s, 2H), 5.97 (d, $J = 1.8$ Hz, 2H), 5.55 (dd, $J = 4.5$, 7.7 Hz, 1H), 4.67 (d, $J = 4.7$ Hz, 1H), 4.54 (dd, $J = 7.3$, 9.0 Hz, 1H), 3.99 (t, $J = 9.9$ Hz, 1H), 3.8 (s, 3H), 3.77 (s, 6H), 3.16–3.07 (m, 1H), 3.04 (dd, $J = 4.7$, 14.1 Hz, 1H); $^{13}$C NMR (75 MHz, CDCl$_3$) $\delta$ (ppm): 174.4, 165.6, 163.2 (d, $J = 249.7$ Hz), 152.6, 148.3, 147.6, 140.7, 140.5, 139.3, 137.2, 135.0, 134.9, 133.6, 132.4, 130.6, 130.1 (d, $J = 8.2$ Hz), 129.2, 122.1, 121.2, 116.3 (d, $J = 22.0$ Hz), 114.1, 111.8, 110.0, 109.3, 108.2, 101.5, 69.2, 60.7, 56.2, 48.0, 43.8, 42.0, 37.7; IR (KBr): 3374.81, 2936.00, 2359.32, 1777.12, 1664.91, 1588.01, 1507.94, 1322.51, 1231.92 cm$^{-1}$; ESI-MS: $m/z$ 702 [M+H]$^+$; HRMS: $m/z$ calcd. for C$_{40}$H$_{33}$FN$_3$O$_8$ 702.22517 [M+H]$^+$, found 702.22460.

### 4.5.5. N-((5S,5aS,8aR,9R)-8-Oxo-9-(3,4,5-trimethoxyphenyl)-5,5a,6,8,8a,9-hexahydrofuro[3′,4′:6,7]naphtho[2,3-d][1,3]dioxol-5-yl)-1-(p-tolyl)-9H-pyrido[3,4-b]indole-3-carboxamide (7e)

White solid; 87% yield; mp: 210–215 °C; [α]$^{25}$$_D$: −83.798 ($c$ = 0.13, CHCl$_3$); $^1$H NMR (300 MHz, CDCl$_3$) $\delta$ (ppm): 8.91(s, 1H), 8.87 (s, 1H), 8.38 (d, $J = 7.7$ Hz, 1H), 8.22 (d, $J = 8.1$ Hz, 1H), 7.77 (d, $J = 7.7$ Hz, 2H), 7.64–7.51 (m, 2H), 7.42–7.34 (m, 3H), 6.85 (s, 1H), 6.55 (s, 1H), 6.34 (s, 2H), 5.96 (d, $J = 3.0$ Hz, 2H), 5.53 (dd, $J = 4.1$, 7.3 Hz, 1H), 4.65 (d, $J = 3.9$ Hz, 1H), 4.53 (dd, $J = 6.0$, 8.1 Hz, 1H), 4.00 (t, $J = 9.0$ Hz, 1H), 3.82 (s, 3H), 3.76 (s, 6H), 3.18–2.98 (m, 2H), 2.44 (s, 3H); $^{13}$C NMR (75 MHz, CDCl$_3$) $\delta$ (ppm): 174.5, 165.7, 152.6, 148.3, 147.6, 141.6,

140.6, 139.5, 139.2, 137.2, 135.0, 134.9, 134.7, 132.3, 130.2, 129.9, 129.2, 129.0, 128.0, 122.2, 122.1, 121.1, 113.8, 111.8, 110.0, 109.3, 108.2, 101.5, 69.2, 60.7, 56.1, 48.0, 43.8, 41.9, 37.7, 21.3; IR (KBr): 3373.06, 2931.76, 2359.42, 1777.00, 1660.86, 1588.78, 1484.95, 1321.52, 1233.35 cm$^{-1}$; ESI-MS: $m/z$ 698 [M+H]$^+$; HRMS: $m/z$ calcd. for C$_{41}$H$_{36}$N$_3$O$_8$ 698.25024 [M+H]$^+$, found 698.24987.

### 4.5.6. 1-(3-Fluorophenyl)-N-((5S,5aS,8aR,9R)-8-oxo-9-(3,4,5-trimethoxyphenyl)-5,5a,6,8,8a,9-hexahydrofuro[3′,4′:6,7]naphtho[2,3-d][1,3]dioxol-5-yl)-9H-pyrido[3,4-b]indole-3-carboxamide (7f)

White solid; 86% yield; mp: 315–320 °C; [α]$^{25}$$_D$: −62.679 ($c$ = 0.11, CHCl$_3$); $^1$H NMR (300 MHz, CDCl$_3$) $\delta$ (ppm): 8.96 (s, 1H), 8.74 (s, 1H), 8.34–8.22 (m, 2H), 7.74–7.53 (m, 5H), 7.41 (t, $J = 6.7$ Hz, 1H), 7.26–7.20 (m, 1H), 6.87 (s, 1H), 6.58 (s, 1H), 6.36 (s, 2H), 5.98 (d, $J = 2.2$ Hz, 2H), 5.55 (dd, $J = 4.5$, 7.5 Hz, 1H), 4.69 (d, $J = 4.5$ Hz, 1H), 4.55 (dd, $J = 6.7$, 8.3 Hz, 1H), 4.00 (t, $J = 9.8$ Hz, 1H), 3.83 (s, 3H), 3.78 (s, 6H), 3.21–2.97 (m, 2H); $^{13}$C NMR (75 MHz, CDCl$_3$) $\delta$ (ppm): 174.4, 165.5, 163.5, 163.2, 163.1 (d, $J = 248.0$ Hz), 162.7, 152.5, 148.3, 147.6, 139.2, 135.0, 134.9, 132.3, 130.8 (d, $J = 8.7$ Hz), 130.7, 129.2 (d, $J = 17.5$ Hz), 123.8, 122.1, 121.9, 121.3, 116.2 (d, $J = 19.7$ Hz), 115.3 (d, $J = 21.9$), 114.4, 111.9, 110.1, 109.2, 108.1, 101.5, 69.2, 60.7, 56.1, 48.1, 43.8, 41.9, 37.6; IR (KBr): 3385.36, 3279.05, 3066.81, 2893.94, 1776.79, 1664.75, 1587.36, 1489.69, 1446.85, 1320.33, 1223.65 cm$^{-1}$; ESI-MS: $m/z$ 702 [M+H]$^+$; HRMS: $m/z$ calcd. for C$_{40}$H$_{33}$FN$_3$O$_8$ 702.22517 [M+H]$^+$, found 702.22491.

### 4.5.7. N-((5S,5aS,8aR,9R)-8-Oxo-9-(3,4,5-trimethoxyphenyl)-5,5a,6,8,8a,9-hexahydrofuro[3′,4′:6,7]naphtho[2,3-d][1,3]dioxol-5-yl)-1-(4-(trifluoromethyl)phenyl)-9H-pyrido[3,4-b]indole-3-carboxamide (7g)

White solid; 88% yield; mp: 333–338 °C; [α]$^{25}$$_D$: −63.425 ($c$ = 0.15, CHCl$_3$); $^1$H NMR (500 MHz, CDCl$_3$) $\delta$ (ppm): 8.98 (s, 1H), 8.79 (bs, 1H), 8.26 (t, $J = 7.7$ Hz, 2H), 8.01 (d, $J = 8.0$ Hz, 2H), 7.86 (d, $J = 8.2$ Hz, 2H), 7.67–7.61 (m, 1H), 7.57 (d, $J = 8.0$ Hz, 1H), 7.42 (t, $J = 7.7$ Hz, 1H), 6.87 (s, 1H), 6.57 (s, 1H), 6.35 (s, 2H), 5.98 (s, 2H), 5.55 (dd, $J = 4.7$, 7.7 Hz, 1H), 4.67 (d, $J = 4.8$ Hz, 1H), 4.55 (dd, $J = 7.3$, 9.1 Hz, 1H), 3.99 (t, $J = 9.4$ Hz, 1H), 3.82 (s, 3H), 3.77 (s, 6H), 3.16–3.08 (m, 1H), 3.03 (dd, $J = 4.8$, 14.3 Hz, 1H); $^{13}$C NMR (75 MHz, CDCl$_3$) $\delta$ (ppm): 174.4, 165.5, 152.5, 148.3, 147.6, 140.8, 140.8, 139.8, 139.3, 137.1, 135.1, 134.9, 132.3, 130.9, 129.3, 129.0, 128.6, 126.2 (q, $J = 4.3$ Hz), 122.1, 121.9, 121.4, 114.6, 111.9, 111.0, 109.2, 108.1, 101.5, 69.1, 60.7, 56.1, 48.1, 43.8, 41.9, 37.6; IR (KBr): 3375.21, 2937.41, 1776.72, 1664.96, 1589.35, 1492.66, 1323.59, 1234.85 cm$^{-1}$; ESI-MS: $m/z$ 752 [M+H]$^+$; HRMS: $m/z$ calcd. for C$_{41}$H$_{33}$F$_3$N$_3$O$_8$ 752.22197 [M+H]$^+$, found 752.22215.

### 4.5.8. 1-(Naphthalen-1-yl)-N-((5S,5aS,8aR,9R)-8-oxo-9-(3,4,5-trimethoxyphenyl)-5,5a,6,8,8a,9-hexahydrofuro[3′,4′:6,7]naphtho[2,3-d][1,3]dioxol-5-yl)-9H-pyrido[3,4-b]indole-3-carboxamide (7h)

White solid; 89% yield; mp: 210–214 °C [α]$^{25}$$_D$: −61.425 ($c$ = 0.18, CHCl$_3$); $^1$H NMR (300 MHz, CDCl$_3$) $\delta$ (ppm): 9.02 (s, 1H), 8.48 (s, 1H), 8.36 (d, $J = 7.5$ Hz, 1H), 8.27 (d, $J = 8.3$ Hz, 1H), 7.93 (dd, $J = 8.3$, 15.1 Hz, 2H), 7.78–7.72 (m, 2H), 7.59 (q, $J = 8.3$, 15.8 Hz, 2H), 7.50 (t, $J = 7.5$ Hz, 1H), 7.45–7.36 (m, 3H), 6.85 (s, 1H), 6.42 (s, 1H), 6.27 (s, 2H), 5.93 (d, $J = 11.3$ Hz, 2H), 5.50 (dd, $J = 4.5$, 7.5 Hz, 1H), 4.53 (t, $J = 8.3$ Hz, 1H), 4.4 (d, $J = 4.5$ Hz, 1H), 4.00 (t, $J = 9.8$ Hz, 1H), 3.79 (s, 3H), 3.71 (s, 6H), 3.13–3.00 (m, 1H), 2.86 (dd, $J = 5.2$, 15.1 Hz, 1H); $^{13}$C NMR (75 MHz, CDCl$_3$) $\delta$ (ppm): 174.6, 165.6, 152.4, 148.0, 147.4, 141.1, 140.6, 138.8, 136.2, 134.8, 134.2, 133.9, 132.1, 131.0, 130.0, 129.5, 129.0, 128.9, 128.5, 127.4, 126.8, 126.3, 125.3, 125.2, 122.0, 121.9, 121.0, 114.1, 111.9, 110.0, 109.1, 107.9, 101.4, 69.2, 60.6, 56.0, 47.9, 43.5, 41.6, 37.6; IR (KBr): 3366.37, 2929.85, 2359.88, 1776.45, 1666.68, 1504.04, 1233.30, 1126.17 cm$^{-1}$; ESI-MS: $m/z$ 734 [M+H]$^+$; HRMS: $m/z$ calcd. for C$_{44}$H$_{36}$N$_3$O$_8$ 734.25024 [M+H]$^+$, found

734.25005.

### 4.5.9. 1-(2,5-Dimethoxyphenyl)-N-((5S,5aS,8aR,9R)-8-oxo-9-(3,4,5-trimethoxyphenyl)-5,5a,6,8,8a,9-hexahydrofuro[3′,4′:6,7]naphtho[2,3-d][1,3]dioxol-5-yl)-9H-pyrido[3,4-b]indole-3-carboxamide (7i)

White solid; 85% yield; mp: 197–202 °C; $[\alpha]^{25}_D$: −82.881 ($c =$ 0.11, CHCl$_3$); $^1$H NMR (500 MHz, CDCl$_3$) δ (ppm): 8.96 (s, 1H), 8.86 (s, 1H), 8.41 (d, $J = 7.4$ Hz, 1H), 8.25 (d, $J = 7.9$ Hz, 1H), 7.60 (t, $J = 8.2$ Hz, 1H), 7.55 (d, $J = 8.0$ Hz, 1H), 7.38 (t, $J = 7.9$ Hz, 1H), 7.20 (d, $J = 3.0$ Hz, 1H), 7.12 (d, $J = 9.0$ Hz, 1H), 7.05 (dd, $J = 3.2, 9.0$ Hz, 1H), 6.89 (s, 1H), 6.56 (s, 1H), 6.35 (s, 2H), 5.96 (dd, $J = 1.2, 13.1$ Hz, 2H), 5.51 (dd, $J = 4.5, 7.4$ Hz, 1H), 4.65 (d, $J = 4.7$ Hz, 1H), 4.56 (dd, $J = 7.0, 9.0$ Hz, 1H), 4.03 (t, $J = 9.3$ Hz, 1H), 3.83 (s, 3H), 3.80 (s, 3H), 3.77 (2 × s, 9H), 3.16–3.07 (m, 1H), 3.04 (dd, $J = 4.7, 14.1$ Hz, 1H); $^{13}$C NMR (75 MHz, CDCl$_3$) δ (ppm): 174.4, 165.8, 153.3, 152.5, 150.7, 147.5, 140.6, 139.1, 138.9, 136.2, 134.9, 132.4, 130.1, 129.3, 128.9, 121.9, 120.8, 116.8, 116.5, 114.5, 113.9, 111.8, 110.1, 109.2, 108.1, 101.4, 69.3, 60.7, 57.6, 56.1, 55.5, 48.2, 43.8, 41.9, 37.7; IR (KBr): 3373.66, 2935.90, 2834.68, 1776.54, 1665.91, 1588.06, 1492.02, 1328.28, 1226.50 cm$^{-1}$; ESI-MS: $m/z$ 744 [M+H]$^+$; HRMS: $m/z$ calcd. for C$_{42}$H$_{38}$N$_3$O$_{10}$ 744.25572 [M+H]$^+$, found 744.25549.

### 4.5.10. 1-(3,4-Difluorophenyl)-N-((5S,5aS,8aR,9R)-8-oxo-9-(3,4,5-trimethoxyphenyl)-5,5a,6,8,8a,9-hexahydrofuro[3′,4′:6,7]naphtho[2,3-d][1,3]dioxol-5-yl)-9H-pyrido[3,4-b]indole-3-carboxamide (7j)

White solid; 89% yield; mp: 290–294 °C; $[\alpha]^{25}_D$: −79.205 ($c =$ 0.15, CHCl$_3$); $^1$H NMR (500 MHz, CDCl$_3$) δ (ppm): 8.97 (s, 1H), 8.80 (s, 1H), 8.23 (t, $J = 8.3$ Hz, 2H), 7.64 (t, $J = 7.1$ Hz, 1H), 7.60 (d, $J = 8.0$ Hz, 1H), 7.45–7.39 (m, 3H), 7.00–6.94 (m, 1H), 6.87 (s, 1H), 6.59 (s, 1H), 6.36 (s, 2H), 5.99 (d, $J = 5.0$ Hz, 2H), 5.54 (dd, $J = 4.5, 7.6$ Hz, 1H), 4.70 (d, $J = 4.7$ Hz, 1H), 4.55 (dd, $J = 7.1, 9.1$ Hz, 1H), 3.99 (t, $J = 9.4$ Hz, 1H), 3.82 (s, 3H), 3.77 (s, 6H), 3.16–3.08 (m, 1H), 3.05 (dd, $J = 4.7, 14.3$ Hz, 1H); $^{13}$C NMR (75 MHz, CDCl$_3$ + DMSO−$d_6$) δ (ppm): 173.8, 165.1, 162.4 (d, $J = 248.1$ Hz), 162.2 (d, $J = 248.6$ Hz), 151.7, 147.2 (d, $J = 45.5$ Hz), 141.4, 140.3, 137.9, 136.3, 134.5 (d, $J = 18.7$ Hz), 131.6, 130.2, 128.4 (d, $J = 36.8$ Hz), 120.8 (d, $J = 7.7$ Hz), 120.0, 113.9, 112.1, 111.2 (d, $J = 25.8$ Hz), 108.9 (d, $J = 55.5$ Hz), 107.5, 103.7, 103.3, 103.0, 100.8, 68.4, 59.8, 55.4, 47.4, 43.2, 41.0, 37.0; IR (KBr): 3386.54, 3273.54, 2906.49, 2841.55, 2359.81, 2341.69, 1778.36, 1665.07, 1597.09, 1448.54 cm$^{-1}$; ESI-MS: $m/z$ 720 [M+H]$^+$; HRMS: $m/z$ calcd. for C$_{40}$H$_{32}$F$_2$N$_3$O$_8$ 720.21575 [M+H]$^+$, found 720.21600.

### 4.5.11. 1-(3-Chlorophenyl)-N-((5S,5aS,8aR,9R)-8-oxo-9-(3,4,5-trimethoxyphenyl)-5,5a,6,8,8a,9-hexahydrofuro[3′,4′:6,7]naphtho[2,3-d][1,3]dioxol-5-yl)-9H-pyrido[3,4-b]indole-3-carboxamide (7k)

White solid; 81% yield; mp: 312–316 °C; $[\alpha]^{25}_D$: −41.860 ($c =$ 0.04, CHCl$_3$); $^1$H NMR (300 MHz, DMSO−$d_6$) δ (ppm): 11.44 (s, 1H), 8.82 (s, 1H), 8.36 (d, $J = 7.7$ Hz, 1H), 8.12 (d, $J = 7.7$ Hz, 1H), 7.88–7.77 (m, 2H), 7.57 (d, $J = 8.1$ Hz, 1H), 7.54–7.37 (m, 3H), 7.30–7.20 (m, 1H), 6.8 (s, 1H), 6.48 (s, 1H), 6.27 (s, 2H), 5.90 (d, $J = 3.3$ Hz, 2H), 5.45 (dd, $J = 4.5, 7.5$ Hz, 1H), 4.58 (d, $J = 4.5$ Hz, 1H), 4.43 (t, $J = 7.5$ Hz, 1H), 3.91 (t, $J = 9.8$ Hz, 1H), 3.70 (s, 3H), 3.68 (s, 6H), 3.19–3.04 (m, 2H); $^{13}$C NMR (75 MHz, CDCl$_3$ + DMSO−$d_6$) δ (ppm): 174.1, 165.5, 152.1, 147.9, 147.2, 141.4, 139.5, 139.3, 138.2, 136.7, 136.5, 134.9, 134.7, 134.2, 131.9, 130.2, 129.9, 128.9, 128.4, 126.7, 121.3, 120.3, 114.0, 112.3, 109.6, 108.9, 107.8, 101.2, 68.9, 60.3, 55.8, 47.7, 43.5, 41.5, 37.4; IR (KBr): 3389.00, 2924.46, 2851.72, 1777.13, 1663.54, 1589.73, 1492.98, 1461.89, 1329.27, 1233.18 cm$^{-1}$; ESI-MS: $m/z$ 718 [M+H]$^+$; HRMS: $m/z$ calcd. for C$_{40}$H$_{33}$ClN$_3$O$_8$ 718.19562 [M+H]$^+$, found 718.19587.

### 4.5.12. 1-(4-Chlorophenyl)-N-((5S,5aS,8aR,9R)-8-oxo-9-(3,4,5-trimethoxyphenyl)-5,5a,6,8,8a,9-hexahydrofuro[3′,4′:6,7]naphtho[2,3-d][1,3]dioxol-5-yl)-9H-pyrido[3,4-b]indole-3-carboxamide (7l)

White solid; 80% yield; mp: 215–220 °C; $[\alpha]^{25}_D$: −76.682 ($c =$ 0.14, CHCl$_3$); $^1$H NMR (500 MHz, CDCl$_3$) δ (ppm): 8.94 (s, 1H), 8.74 (s, 1H), 8.29 (d, $J = 7.7$ Hz, 1H), 8.24 (d, $J = 7.7$ Hz, 1H), 7.82 (d, $J = 8.3$ Hz, 2H), 7.66–7.60 (m, 1H), 7.59–7.55 (m, 3H), 7.42–7.38 (m, 1H), 6.86 (s, 1H), 6.57 (s, 1H), 6.35 (s, 2H), 5.98 (s, 2H), 5.54 (dd, $J = 4.5, 7.7$ Hz, 1H), 4.67 (d, $J = 4.8$ Hz, 1H), 4.54 (dd, $J = 7.3, 9.1$ Hz, 1H), 3.99 (t, $J = 9.4$ Hz, 1H), 3.82 (s, 3H), 3.77 (s, 6H), 3.15–3.07 (m, 1H), 3.03 (dd, $J = 4.8, 14.4$ Hz, 1H); $^{13}$C NMR (75 MHz, CDCl$_3$) δ (ppm): 174.5, 165.6, 152.5, 148.3, 147.6, 140.8, 140.2, 139.2, 137.1, 135.9, 135.3, 135.0, 134.9, 132.3, 130.6, 129.5, 129.4, 129.2, 129.1, 122.1, 122.0, 121.2, 114.2, 111.9, 110.0, 109.2, 108.2, 101.5, 69.2, 60.7, 56.1, 48.1, 43.8, 42.0, 37.7; IR (KBr): 3363.54, 2933.74, 2359.78, 1776.21, 1661.25, 1588.90, 1491.26, 1321.61, 1233.44 cm$^{-1}$; ESI-MS: $m/z$ 718 [M+H]$^+$; HRMS: $m/z$ calcd. for C$_{40}$H$_{33}$ClN$_3$O$_8$ 718.19562 [M+H]$^+$, found 718.19565.

### 4.5.13. 1-(2-Methoxyphenyl)-N-((5S,5aS,8aR,9R)-8-oxo-9-(3,4,5-trimethoxyphenyl)-5,5a,6,8,8a,9-hexahydrofuro[3′,4′:6,7]naphtho[2,3-d][1,3]dioxol-5-yl)-9H-pyrido[3,4-b]indole-3-carboxamide (7m)

White solid; 80% yield; mp: 175–180 °C; $[\alpha]^{25}_D$: −92.488 ($c =$ 0.06, CHCl$_3$); $^1$H NMR (500 MHz, CDCl$_3$) δ (ppm): 8.96 (s, 1H), 8.71 (s, 1H), 8.39 (d, $J = 7.9$ Hz, 1H), 8.23 (d, $J = 7.7$ Hz, 1H), 7.63 (dd, $J = 1.2, 7.4$ Hz, 1H), 7.59 (t, $J = 7.7$ Hz, 1H), 7.55–7.50 (m, 2H), 7.36 (t, $J = 7.6$ Hz, 1H), 7.20–7.14 (m, 2H), 6.87 (s, 1H), 6.54 (s, 1H), 6.35 (s, 2H), 5.96 (d, $J = 7.1$ Hz, 2H), 5.54 (dd, $J = 4.5, 7.7$ Hz, 1H), 4.64 (d, $J = 4.7$ Hz, 1H), 4.56–4.52 (m, 1H), 4.01 (t, $J = 9.6$ Hz, 1H), 3.87 (s, 3H), 3.82 (s, 3H), 3.77 (s, 6H), 3.12–3.06 (m, 1H), 3.03 (dd, $J = 4.7, 14.3$ Hz, 1H); $^{13}$C NMR (75 MHz, CDCl$_3$) δ (ppm): 174.5, 165.8, 156.5, 152.5, 148.2, 147.5, 140.5, 139.5, 138.9, 137.0, 136.2, 134.9, 132.4, 132.3, 130.7, 129.7, 129.2, 128.8, 126.7, 122.0, 121.7, 120.7, 113.9, 112.0, 111.7, 109.9, 109.3, 108.0, 101.4, 69.2, 60.7, 56.2, 56.1, 47.9, 43.8, 41.8, 37.6; IR (KBr): 3363.08, 2926.21, 2836.52, 2363.35, 1775.32, 1665.79. 1587.42, 1489.80, 1320.34 cm$^{-1}$; ESI-MS: $m/z$ 714 [M+H]$^+$; HRMS: $m/z$ calcd. for C$_{41}$H$_{36}$N$_3$O$_9$ 714.24515 [M+H]$^+$, found 714.24414.

### 4.5.14. N-((5S,5aS,8aR,9R)-8-Oxo-9-(3,4,5-trimethoxyphenyl)-5,5a,6,8,8a,9-hexahydrofuro[3′,4′:6,7]naphtho[2,3-d][1,3]dioxol-5-yl)-1-phenyl-9H-pyrido[3,4-b]indole-3-carboxamide (7n)

White solid; 89% yield; mp: 314–318 °C; $[\alpha]^{25}_D$: −61.655 ($c =$ 0.14, CHCl$_3$); $^1$H NMR (500 MHz, CDCl$_3$) δ (ppm): 8.94 (s, 1H), 8.72 (s, 1H), 8.36 (d, $J = 7.9$ Hz, 1H), 8.25 (d, $J = 7.9$ Hz, 1H), 7.90–7.86 (m, 2H), 7.64–7.59 (m, 3H), 7.57–7.53 (m, 2H), 7.42–7.38 (m, 1H), 6.87 (s, 1H), 6.56 (s, 1H), 6.35 (s, 2H), 5.97 (dd, $J = 1.2, 6.4$ Hz, 2H), 5.55 (dd, $J = 4.4, 7.7$ Hz, 1H), 4.67 (d, $J = 4.7$ Hz, 1H), 4.54 (dd, $J = 7.0, 9.0$ Hz, 1H), 4.00 (t, $J = 9.3$ Hz, 1H), 3.82 (s, 3H), 3.77 (s, 6H), 3.16–3.08 (m, 1H), 3.05 (dd, $J = 4.7, 14.3$ Hz, 1H); $^{13}$C NMR (75 MHz, CDCl$_3$) δ (ppm): 174.5, 165.7, 152.5, 1448.2, 1447.6, 141.4, 140.7, 139.2, 137.5, 137.1, 135.1, 134.9, 132.3, 130.4, 129.2, 129.1, 129.0, 128.2, 122.0, 121.1, 114.0, 111.8, 110.0, 109.3, 108.2, 101.4, 69.2, 60.7, 56.2, 48.0, 43.8, 41.9, 37.7; IR (KBr): 3375.91, 2906.72, 2838.34, 2359.25, 1776.23, 1664.68, 1587.65, 1493.72, 1326.28, 1231.98 cm$^{-1}$; ESI-MS: $m/z$ 684 [M+H]$^+$; HRMS: $m/z$ calcd. for C$_{40}$H$_{34}$N$_3$O$_8$ 684.23459 [M+H]$^+$, found 684.23421.

### 4.5.15. N-((5S,5aS,8aR,9R)-8-Oxo-9-(3,4,5-trimethoxyphenyl)-5,5a,6,8,8a,9-hexahydrofuro[3′,4′:6,7]naphtho[2,3-d][1,3]dioxol-5-yl)-1-(pyridin-3-yl)-9H-pyrido[3,4-b]indole-3-carboxamide (7o)

White solid; 83% yield; mp: 210–215 °C; $[\alpha]^{25}_D$: −66.417 ($c =$ 0.12, CHCl$_3$); $^1$H NMR (500 MHz, CDCl$_3$) δ (ppm): 10.41 (s, 1H), 9.34 (d, $J = 1.5$ Hz, 1H), 9.01 (s, 1H), 8.67 (dd, $J = 1.5, 4.8$ Hz, 1H),

8.31−8.22 (m, 3H), 7.64−7.52 (m, 3H), 7.43−7.39 (m, 1H), 6.88 (s, 1H), 6.58 (s, 1H), 6.35 (s, 2H), 5.98 (d, $J = 1.6$ Hz, 2H), 5.56 (dd, $J = 4.5, 7.7$ Hz, 1H), 4.68 (d, $J = 4.7$ Hz, 1H), 4.56 (dd, $J = 7.3, 9.1$ Hz, 1H), 4.01 (t, $J = 9.4$ Hz, 1H), 3.83 (s, 3H), 3.77 (s, 6H), 3.17−3.09 (m, 1H), 3.05 (dd, $J = 4.8, 14.3$ Hz, 1H); $^{13}$C NMR (75 MHz, CDCl$_3$) $\delta$ (ppm): 174.4, 165.5, 152.6, 149.2, 148.8, 148.3, 147.6, 141.7, 139.2, 137.9, 137.2, 136.7, 135.6, 134.8, 134.2, 132.4, 131.0, 129.3, 124.4, 129.2, 122.0, 121.8, 121.1, 114.8, 112.1, 110.0, 109.3, 108.2, 101.5, 69.2, 60.7, 56.1, 48.1, 43.8, 42.0, 37.6; IR (KBr): 3372.38, 2935.22, 2359.45, 1776.36, 1660.54, 1588.61, 1482.84, 1330.73, 1233.79 cm$^{-1}$; ESI-MS: $m/z$ 685 [M+H]$^+$; HRMS: $m/z$ calcd. for C$_{39}$H$_{33}$N$_4$O$_8$ 685.22984 [M+H]$^+$, found 685.22920.

### 4.5.16. N-((5S,5aS,8aR,9R)-8-oxo-9-(3,4,5-trimethoxyphenyl)-5,5a,6,8,8a,9-hexahydrofuro[3′,4′:6,7]naphtho[2,3-d][1,3]dioxol-5-yl)-1-(3-phenoxyphenyl)-9H-pyrido[3,4-b]indole-3-carboxamide (7p)

White solid; 89% yield; mp: 197−200 °C; [α]$^{25}$$_D$: −68.652 ($c = 0.14$, CHCl$_3$); $^1$H NMR (500 MHz, CDCl$_3$) $\delta$ (ppm): 8.93 (s, 1H), 8.73 (s, 1H), 8.28 (d, $J = 7.9$ Hz, 1H), 8.23 (d, $J = 7.9$ Hz, 1H), 7.64−7.59 (m, 2H), 7.55 (t, $J = 7.6$ Hz, 2H), 7.51 (t, $J = 2.2$ Hz, 1H), 7.41−7.34 (m, 3H), 7.20−7.13 (m, 2H), 7.04 (dd, $J = 1.0, 8.6$ Hz, 2H), 6.86 (s, 1H), 6.58 (s, 1H), 6.36 (s, 2H), 5.97 (dd, $J = 1.2, 9.6$ Hz, 2H), 5.54 (dd, $J = 4.7, 7.7$ Hz, 1H), 4.68 (d, $J = 4.8$ Hz, 1H), 4.53 (dd, $J = 7.4, 9.1$ Hz, 1H), 3.97 (dd, $J = 9.4, 10.6$ Hz, 1H), 3.83 (s, 3H), 3.78 (s, 6H), 3.15−3.06 (m, 1H), 3.00 (dd, $J = 4.8, 14.3$ Hz, 1H); $^{13}$C NMR (75 MHz, CDCl$_3$) $\delta$ (ppm): 174.4, 165.6, 158.2, 156.4, 152.5, 148.2, 147.5, 140.6, 139.1, 137.1, 134.9, 132.3, 130.6, 130.5, 129.8, 129.2, 129.1, 123.9, 122.6, 122.0, 121.9, 121.1, 119.2, 119.0, 118.1, 114.2, 111.8, 110.0, 109.2, 108.1, 101.4, 69.1, 60.7, 56.1, 48.0, 43.8, 41.9, 37.6; IR (KBr): 3347.51, 2903.88, 2361.01, 1775.65, 1662.69, 1581.60, 1486.75, 1439.03, 1320.10, 123.42 cm$^{-1}$; ESI-MS: $m/z$ 776 [M+H]$^+$; HRMS: $m/z$ calcd. for C$_{46}$H$_{38}$N$_3$O$_9$ 776.26080 [M+H]$^+$, found 776.26049.

### 4.5.17. 1-(3,4-Dimethoxyphenyl)-N-((5S,5aS,8aR,9R)-8-oxo-9-(3,4,5-trimethoxyphenyl)-5,5a,6,8,8a,9-hexahydrofuro[3′,4′:6,7]naphtho[2,3-d][1,3]dioxol-5-yl)-9H-pyrido[3,4-b]indole-3-carboxamide (7q)

White solid; 81% yield; mp: 195−200 °C; [α]$^{25}$$_D$: −62.679 ($c = 0.06$, CHCl$_3$); $^1$H NMR (500 MHz, CDCl$_3$) $\delta$ (ppm): 8.89 (s, 1H), 8.75 (s, 1H), 8.40 (d, $J = 7.4$ Hz, 1H), 8.24 (d, $J = 7.8$ Hz, 1H), 7.62 (t, $J = 7.4$ Hz, 1H), 7.56 (d, $J = 8.0$ Hz, 1H), 7.47 (dd, $J = 1.7, 8.1$ Hz, 1H), 7.39 (t, $J = 7.5$ Hz, 1H), 7.37 (d, $J = 1.7$ Hz, 1H), 7.07 (d, $J = 8.3$ Hz, 1H), 6.90 (s, 1H), 6.57 (s, 1H), 6.35 (s, 2H), 5.96 (d, $J = 12.2$ Hz, 2H), 5.49 (dd, $J = 4.4, 7.2$ Hz, 1H), 4.65 (d, $J = 4.7$ Hz, 1H), 4.56 (dd, $J = 7.4, 8.9$ Hz, 1H), 4.03 (t, $J = 9.7$ Hz, 1H), 3.97 (s, 3H), 3.89 (s, 3H), 3.82 (s, 3H), 3.77 (s, 6H), 3.16−3.08 (m, 1H), 3.04 (dd, $J = 4.7, 14.1$ Hz, 1H); $^{13}$C NMR (75 MHz, CDCl$_3$) $\delta$ (ppm): 174.4, 165.8, 152.5, 150.1, 149.6, 148.2, 147.5, 141.2, 140.6, 139.1, 137.1, 135.0, 134.8, 132.4, 130.3, 130.2, 129.3, 129.0, 122.2, 121.1, 120.3, 113.6, 111.8, 111.6, 111.4, 110.1, 109.2, 108.1, 101.5, 69.3, 60.7, 56.1, 56.0, 55.9, 48.2, 43.8, 41.9, 37.8; IR (KBr): 3359.82, 2931.73, 2836.63, 1776.63, 1665.57, 1588.31, 1512.45, 1485.38, 1329.72, 1234.69 cm$^{-1}$; MS (ESI): 744 [M+H]$^+$; HRMS(ESI): $m/z$ calcd. for C$_{42}$H$_{38}$N$_3$O$_{10}$ 744.25572, found 744.25549 [M+H]$^+$.

## 4.6. Biology

### 4.6.1. Cytotoxic assay

The cytotoxic activity of the **7a–q** was determined using MTT assay [24]. $1 \times 10^4$ cells/well were seeded in 100 μl DMEM or MEM, supplemented with 10% FBS in each well of 96-well microculture plates and incubated for 24 h at 37 °C in a CO$_2$ incubator. After 24 h of incubation, all the synthesized congeners were added to the cells and incubated for 48 h. After 48 h of drug treatment, 10 μl MTT (3-(4, 5-dimethylthiazol-2-yl)-2, 5-diphenyl tetrazolium bromide) (5 mg/mL) was added to each well and the plates were further incubated for 4 h. Then the supernatant from each well was carefully removed, the formazon crystals were dissolved in 100 μl of DMSO and absorbance at 570 nm wavelength was recorded.

### 4.6.2. Cell cycle analysis

Flow cytometric analysis (FACS) was performed to evaluate the distribution of the cells in different cell cycle phases. DU-145 cells were incubated with **7i** and **7j** congeners at 1 μM concentration for 48 h. Untreated cells were considered as control sample. Untreated and treated cells were harvested, washed with PBS, fixed in ice cold 70% ethanol and stained with propidium iodide (Sigma Aldrich). Cell cycle was performed by using Becton Dickinson FACS Caliber (USA).

### 4.6.3. DNA topo II inhibition assay

In order to determine the effect of **7i** and **7j** in topoisomerase II inhibition and the formation efficiency of decatenated kDNA was studied using the protocol mentioned in topoisomerase II Drug Screening Kit (TG 1009, Topogen, USA). Topoisomerase II inhibition was assayed using the ATP dependent decatenation of kDNA and all the reactions were carried out in 20 μl and contained 120 mM KCl, 50 mM Tris−HCl, pH 8, 10 mM MgCl$_2$, 0.5 mM dithiothreitol, 0.5 mM ATP, 30 mg/ml bovine serum albumin, 200−300 ng of kDNA, and topoisomerase II. The amount of topoisomerase II (5 units) was adjusted in preliminary experiments to decatenate approximately 100% of the kDNA under these assay conditions. The reactions samples were incubated at 37 °C for 30 min and terminated by the addition of 2 μl of a stop buffer containing 10% (w/v) SDS and 2 μl of 0.5 mg/ml proteinase-K and incubated for 10 min at 37 °C. After completion of the reaction, the products in the reaction mixture were separated by 1% agarose gel and visualized after staining with ethidium bromide (0.2 l g/ml). The gels were run at 100 V for about 40 min and visualized under UV transillumination (BIO RAD gel doc XR$^+$, USA).

### 4.6.4. Comet assay

The DU-145 cells were seeded in 60 mm dishes and were treated with etoposide and 7i and 7j hybrids at a concentration for 10 μM concentration for 24 h. Briefly, about 25,000 cells were embedded in agarose and deposited in microscope slides. The slides were incubated for 2 h in lysis solution (2.5 M NaCl, 100 mM EDTA, 10 mM Tris, pH 10, 10% DMSO, 1% Triton X-100) followed by 3 washes in neutralizing buffer (0.4 M Tris−HCl, pH 7.5). Electrophoresis was carried out for 20 min at 40 V in 0.5% TBE buffer (pH 8). During electrophoresis the damaged DNA migrates away from the nucleus towards anode. Slides were then stained with a 10 mg/mL propidium iodide solution for 30 min. Images from were taken in fluorescent microscope at 20x magnification.

### 4.6.5. DNA binding studies

#### 4.6.5.1. UV−visible spectroscopy.
UV−visible absorption spectra were recorded using Perkin Elmer ABI 35 Lambda Spectrophotometer (Waltham, MA, USA) at 25 °C. All the titrations were carried out in polystyrene cuvettes to minimize binding of conjugates to the surface of the cuvettes. Then, 50 μM of **7i** and **7j** stock solution was prepared in DMSO and 25.0 μM of CT-DNA in 100 mM Tris-HCl (pH 7.0). About 1 ml of 25.0 μM conjugate solution was taken in a 1 cm path length cuvette and 5 μl of DNA was added each titration. All the stock solutions used were freshly prepared before commencing the experiment, titration was carried out until saturation of absorbance occurs and the absorption spectra recorded in the range of 200 nm to 400 nm.

*M. Sathish et al. / European Journal of Medicinal Chemistry 144 (2018) 557–571*

*4.6.5.2. Fluorescnece titration.* Fluorescence emission spectra were measured at 25 °C using a Hitachi F7000 spectrofluorimeter (Maryland, USA) using a 1 cm path length quartz cuvette. Initially, quartz cuvettes was thoroughly washed with distilled water and dilute nitric acid (approximately 0.1 N) to minimize non-specific binding of the conjugates to the surface of the cuvette. Throughout the fluorescence experiment, concentration of the **7i** and **7j** were kept constant (10 μM) and titrated with equally increasing concentrations of CT-DNA (multiples of 0.5 μM). Fluorescence spectra were recorded after each addition of CT-DNA to the fluorescent cuvette. The complexes were excited at 230 nm and emission spectra for each titration was recorded up to 600 nm. The average of three scans was taken after recording three individual spectrum.

*4.6.5.3. Circular dichorism (CD) studies.* DNA conformational studies were carried out on a JASCO 815 CD spectropolarimeter (Jasco, Tokyo, Japan). CD Spectroscopic studies were performed to study the change in DNA conformation brought by **7i** and **7j** molecules on interaction with CT-DNA at micro molar concentration range. The CT-DNA solution was prepared in 100 mM *Tris*-HCl (pH 7.0) and 10 μM of CT-DNA added about 10.0 μM and 20 μM (1:1 and 1:2 ratio of DNA:complex) of each solution containing **7i** and **7j** molecules was added and CD spectra was recorded from 200 nm to 350 nm using 1 mm path length cuvette. The spectra were averaged over 3 scans.

*4.6.6. Docking studies*

The active congeners **7i** and **7j** were built in Maestro 10.4 [35], prepared using Ligprep 3.6 [36] and geometrically minimized with Macromodel 11.0 [37] followed by conformational analysis. Truncated Newton Conjugate Gradient minimization was used with 500 iterations and convergence threshold of 0.05 kJ/mol. The DNA topoisomerase-IIα (PDB ID: 1ZXM) and d(CGCGAATTCGCG)$_2$ (PDB ID: 1DNH) duplex were prepared using protein preparation wizard [38]. The Glide XP 6.9 [39] algorithm was employed using a grid box volume of 10 × 10 × 10 Å. Briefly, Glide approximates a systematic search of positions, orientations and conformations of the ligand in the receptor binding site using a series of hierarchical filters. Upon completion of each docking calculation, 100 poses per ligand were generated and the best docked structure was chosen using a GlideScore (Gscore) function.

**Acknowledgments**

**Appendix A. Supplementary data**

Supplementary data related to this article can be found at https://doi.org/10.1016/j.ejmech.2017.12.055.

**References**

[1] (a) K. Chikamori, A.G. Grozav, T. Kozuki, D. Grabowski, R. Ganapathi, M.K. Ganapathi, Curr. Cancer. Drug Targets 10 (2010) 758;
(b) M.S. Christodoulou, M. Zarate, F. Ricci, G. Damia, S. Pieraccini, F. Dapiaggi, M. Sironi, L. Lo Presti, A.N. García-Argáez, L. Dalla Via, Passarella, D. Eur. J. Med. Chem. 118 (2016) 79;
(c) H.B. Kwon, C. Park, K.H. Jeon, E. Lee, S.E. Park, K.Y. Jun, T.M. Kadayat, P. Thapa, R. Karki, Y. Na, M.S. Park, S.B. Rho, E.S. Lee, Y. Kwon, J. Med. Chem. 58 (2015) 1100;
(d) B.L. Yao, Y.W. Mai, S.B. Chen, H.T. Xie, P.F. Yao, T.M. Ou, J.H. Tan, H.G. Wang, D. Li, S.L. Huang, L.Q. Gu, Z.S. Huang, Eur Eur. J. Med. Chem. 92 (2015) 540;
(e) C. Bailly, Chem. Rev. 112 (2012) 3611;
(f) W. Luniewski, J. Wietrzyk, J. Godlewska, M. Switalska, M. Piskozub, W. Peczynska-Czoch, L. Kaczmarek, Bioorg. Med. Chem. Lett. 22 (2012) 6103;
(g) N. Ferri, T. Radice, M. Antonino, E.M. Beccalli, S. Tinelli, F. Zunino, A. Corsini, G. Pratesi, E.M. Ragg, M.L. Gelmi, A. Contini, Bioorg. Med. Chem. 19 (2011) 5291;
(h) A. Wu, Y. Xu, X. Qian, Monatsh. Chem. 141 (2010) 893;
(i) Y. Pommier, E. Leo, H. Zhang, C. Marchand, Chem. Biol. 17 (2010) 421;
(j) N. Ferri, E.M. Beccalli, A. Contini, A. Corsini, M. Antonino, T. Radice, G. Pratesi, S. Tinelli, F. Zunino, M.L. Gelmi, Biorg. Med. Chem. 16 (2008) 1691;
(k) A. Kamal, B.S. Narayan Reddy, G. Suresh Kumar Reddy, G. Ramesh, Bioorg. Med. Chem. Lett. 12 (2002) 1933.
[2] J.L. Nitiss, Nat. Rev. Canc. 9 (2009) 338.
[3] M. Iwai, A. Hara, T. Andoh, R. Ishida, FEBS Lett. 406 (1997) 267.
[4] Y. Pommier, E. Leo, H. Zhang, C. Marchand, Chem. Biol. 17 (2010) 421.
[5] Y. You, Curr. Pharmaceut. Des. 11 (2005) 1695.
[6] (a) F. Cortese, B. Bhattacharyya, B. Wolf, J. Biol. Chem. 252 (1977) 1134;
(b) S. Desbène, S. Giorgi-Renault, Curr. Med. Chem. Anti Canc. Agents 1 (2001) 71.
[7] (a) S.A. Beers, Y. Imakura, H.J. Dai, D.H. Li, Y.C. Cheng, K.H. Lee, J. Nat. Prod. 51 (1988) 901;
(b) H. Laatsch, B.P. Ernst, M. Noltemeyer, Liebigs Ann. (1996) 731.
[8] K.R. Hande, Eur. J. Canc. 34 (1998) 1514.
[9] H. Emmengger, H. Stahelin, J. Rutschmann, A. von Wartburg, Altorient. Forsch. 11 (1961) 327.
[10] H.F. Stahelin, A. von Wartburg, Canc. Res. 51 (1991) 5.
[11] L.P. Schacter, L.N. Igwemezie, M. Seyedsadr, Canc. Chemother. Pharmacol. 34 (1994) 58.
[12] (a) . https://en.wikipedia.org/wiki/Etoposide;
(b) . https://en.wikipedia.org/wiki/Teniposide#Side_effects.
[13] K. Patel, M. Gadewar, R. Tripathi, S.K. Prasad, Patel Dinesh Kumar, Asian Pac. J. Trop. Biomed. 2 (2012) 660.
[14] (a) E.J. Massaro, Handbook of Neurotoxicology, Humana Press, 2002, p. 237;
(b) N. Devi, Sunit Kumar, S.K. Pandey, V. Singh, Asian J. Org. Chem http://doi.org./10.1002/ajoc.201700477.
[15] J. Osorio Edison, M. Robledo Sara, Bastida Jaume, Alkaloids - Chem. Biol. (2008) 113.
[16] (a) S. Xiao, W. Lin, C. Wang, M. Yang, Bioorg. Med. Chem. Lett. 11 (2001) 437;
(b) K. Hayashi, M. Nagao, T. Sugimura, Nucleic Acids Res. 4 (1977) 3679.
[17] J.I. Trujillo, M.J. Meyers, D.R. Anderson, S. Hegde, M.W. Mahoney, W.F. Vernier, I.P. Buchler, K.K. Wu, S. Yang, S.J. Hartmann, D.B. Reitz, Bioorg. Med. Chem. Lett. 17 (2007) 4657.
[18] (a) A.M. Deveau, M.A. Labroli, C.M. Dieckhaus, M.T. Barthen, K.S. Smith, T.L. Macdonald, Bioorg. Med. Chem. Lett. 11 (2001) 1251;
(b) M. Zhao, L. Bi, W. Wang, C. Wang, Bioorg. Med. Chem. 14 (2006) 6998;
(c) R. Chaniyara, S. Tala, C.W. Chen, X. Zang, R. Kakadiya, L.F. Lin, C.H. Chen, S.I. Chien, T.C. Chou, T.H. Tsai, T.C. Lee, A. Shah, T.L. Su, J. Med. Chem. 56 (2013) 1544.
[19] P.A. Barsanti, W. Wang, Z. Ni, D. Duhl, N. Brammeier, E. Martin, Bioorg. Med. Chem. Lett. 20 (2010) 157.
[20] (a) Y. Song, J. Wang, S.F. Teng, D. Kesuma, Y. Deng, J. Duan, J.H. Wang, R.Z. Qi, M.M. Sim, Bioorg. Med. Chem. Lett. 12 (2002) 1129;
(b) Y. Song, D. Kesuma, J. Wang, Y. Deng, J. Duan, J.H. Wang, R.Z. Qi, Biochem. Biophys. Res. Commun. 317 (2004) 128.
[21] R. Martinez, L. Chacon-Garcia, Curr. Med. Chem. 12 (2005) 127.
[22] J.S. Madalengoitia, J.J. Tepe, K.A. Werbovetz, E.K. Lehnert, T.L. Macdonald, Bioorg. Med. Chem. 5 (1997) 1807.
[23] (a) A. Kamal, M. Sathish, V.L. Nayak, V. Srinivasulu, B. Kavitha, Y. Tangella, D. Thummuri, C. Bagul, N. Shankaraiah, N. Nagesh, Bioorg. Med. Chem. 23 (2015) 5511;
(b) A. Kamal, A.A. Kumar, M. Arifuddin, S.G. Dastidar, Bioorg. Med. Chem. 11 (2003) 5135.
[24] J.K. Wilson, J.M. Sargent, A.W. Elgie, J.G. Hill, C.G. Taylor, Br. J. Canc. 62 (1990) 189.
[25] (a) C. Nam, K. Doi, H. Nakayama, Histol. Histopathol. 25 (2010) 485;
(b) H.M. Robinson, S. Bratlie-Thoresen, R. Brown, D.A. Gillespie, Cell Cycle 6 (2007) 1265.
[26] J.L. Nitiss, W.T. Beck, Eur. J. Canc. 32A (1996) 958.
[27] (a) Y. Pommier, E. Leo, H.L. Zhang, Chem. Biol. 17 (2010) 421;
(b) G. Boos, H. Stopper, Toxicol. Lett. 116 (2000) 7.
[28] B.D. Wang, Z.Y. Yang, P. Crewdson, D.Q. Wang, J. Inorg. Biochem. 101 (2007) 1492.
[29] E.C. Long, J.K. Barton, Acc. Chem. Res. 23 (1990) 271.
[30] J. Wu, M. Zhao, K. Qian, K.-H. Lee, S. Morris–Natschke, S. Peng, Eur. J. Med. Chem. 44 (2009) 4153.
[31] H. Fukuda, M. Katahira, N. Tsuchiya, Y. Enokizono, T. Sugimura, M. Nagao, H. Nakagama, Proc. Natl. Acad. Sci. Unit. States Am. 99 (2002), 12685.
[32] V.A. Barbosa, A.S. Formagio, F.C. Savariz, M.A. Foglio, H.M. Spindola, J.E. de Carvalho, E. Meyer, M.H. Sarragiotto, Bioorg. Med. Chem. 19 (2011) 6400.
[33] (a) A. Kamal, Y. Tangella, K.L. Manasa, M. Sathish, V. Srinivasulu, J. Chetna,

A. Alarifi, Org. Biomol. Chem. 13 (2015) 8652;
(b) A. Kamal, M. Sathish, A.V.G. Prasanthi, J. Chetna, Y. Tangella, V. Srinivasulu, N. Shankaraiah, A. Alarifi, RSC Adv. 5 (2015), 90121.

[34] A. Kamal, V. Srinivasulu, V.L. Nayak, M. Sathish, N. Shankaraiah, C. Bagul, N.V. Reddy, N. Rangaraj, N. Nagesh, ChemMedChem 9 (2014) 2084.

[35] Maestro, Schrödinger, LLC, New York, NY, 2015.

[36] Schrödinger Release 2015-4: LigPrep, Version 3.6, Schrödinger, LLC, New York, NY, 2015.

[37] MacroModel, Schrödinger, LLC, New York, NY, 2015.

[38] Protein Preparation Wizard, Schrödinger, LLC, New York, NY, 2015.

[39] Small-molecule Drug Discovery Suite 2015-4: Glide, Version 6.9, Schrödinger, LLC, New York, NY, 2015.